

Accepted by ApJ

The Variability and Period Analysis for the BL Lac AO 0235+164

J.H. Fan^{1,21}, O. Kurtanidze^{3,4}, Y. Liu^{1,2}, X. Liu⁵, J.H. Yang⁶, G.M. Richter⁷, M.G. Nikolashvili³, S. O. Kurtanidze³, H. T. Wang⁸, M. Sasada⁹, A. Y. Zhou¹⁰, C. Lin^{1,2}, Y. H. Yuan^{1,2}, Y. T. Zhang^{1,2}, D. Constantin^{1,2}

ABSTRACT

Variability is one of the extreme observational properties of BL Lacertae objects. AO 0235+164 is a well studied BL Lac through the whole electro-magnetic wavebands. In the present work, we show its optical R band photometric observations carried out during the period of Nov, 2006 to Dec. 2012 using the Ap6E CCD camera attached to the primary focus of the 70 – cm meniscus telescope at Abastumani Observatory, Georgia. It shows a large variation of $\Delta R = 4.88$ mag (14.19 - 19.07 mag) and a short time scale of $\Delta T_v = 73.5$ min during our monitoring period. During the period of Dec. 2006 to Nov. 2009, we made radio observations of the source using the 25-m radio telescope at Xinjiang Astronomical Observatory. When a discrete correlation function (DCF) is adopted to the optical and radio observations, we found that the optical variation leads the radio variation by 23.2 ± 12.9 days.

¹Center for Astrophysics, Guangzhou University, Guangzhou 510006, China

²Astronomy Science and Technology Research Laboratory of Department of Education of Guangdong Province, Guangzhou 510006, China

³Abastumani Observatory, Mt. Kanobili, 0301 Abastumani, Georgia

⁴Engelhardt Astronomical Observatory, Kazan Federal University, Tatarstan, Russia

⁵Xinjiang Astronomical Observatory, Chinese Academy of Sciences, Urumqi 830011, China

⁶Dept of Physics and Electronics Science, Hunan University of Arts and Science, Changde, 415000, China

⁷Astrophysikalisches Institut Potsdam, An der Sternwarte 16, 14482 Potsdam, Germany

⁸Faculty of Physics and Electronic Information, LangFang Teacher's College, China

⁹Department of Astronomy, Boston University, USA

¹⁰National Astronomical Observatory, Chinese Academy of Sciences, Beijing, China

Subject headings: Galaxies: BL Lacertae Objects: individual (AO 0235+164); photometry: Variability

1. Introduction

Blazars as a very extreme subclass of active galactic nuclei(AGNs) show special observation properties, such as luminous emissions, rapid and high amplitude variability, high and variable polarization, strong and variable γ -ray emissions, strong emission line feature or no-emission line features at all, or superluminal motions etc. Blazars have two subclasses: BL Lacertae objects (BLs) and flat spectrum radio quasars (FSRQs). The major difference for the two subclasses is their difference in emission line features with FSRQs showing strong emission line features while BLs showing very weak emission lines or no emission lines at all. BLs can be divided into radio selected BLs (RBLs) and X-ray selected BLs (XBLs) from survey, or low frequency-peaked BL Lacertae objects (LBLs, $\log\nu_p < 15$ Hz) and high frequency-peaked BL Lacertae objects (HBL, $\log\nu_p > 15$ Hz) from the synchrotron peak frequency in their spectral energy distribution (SED) (Padovani & Giommi 1995; Urry & Padovani 1995). To avoid confusion, Abdo et al. (2010a) extended the definition to all types of non-thermal dominated AGNs using new acronyms as low synchrotron peaked blazars-LSP, intermediate synchrotron peaked blazars-ISP, and high synchrotron peaked blazars-HSP with LSP showing their peak synchrotron powers in far-IR or IR band ($\log\nu_p < 14$ Hz); ISP showing their peak synchrotron emissions in the frequency range of $\log\nu_p = 14 \sim 15$ Hz; and HSP showing their peak synchrotron powers at frequency of $\log\nu_p > 15$ Hz. Very recently, we calculated the SEDs using $\log(\nu F_\nu) = P_1(\log\nu - P_2)^2 + P_3$ for a sample of 1425 Fermi blazars. Synchrotron peak frequency ($\log\nu_p$), spectral curvature (P_1), peak flux ($\nu_p F_{\nu_p}$), and integrated flux (νF_ν) are successfully obtained for 1392 blazars. The "Bayesian classification" is adopted to $\log\nu_p$ in the rest frame for 999 blazars with available redshift and the results show that 3 components are enough to fit the $\log\nu_p$ distribution. Therefore, we proposed LSP with $\log\nu_p < 14$ Hz; ISP with $\log\nu_p = 14 \sim 15.3$ Hz; HSP with $\log\nu_p > 15.3$ Hz (Fan et al. 2016).

One of the most important results of the Fermi/LAT is the discovery of blazars, which emit most of their bolometric luminosity in the high energy range γ -rays ($0.1 \sim 100$ GeV)

¹email:fjh@gzhu.edu.cn

(Abdo et al. 2010b; Ackermann et al. 2012; Nolan et al. 2012; Ackermann et al. 2015). The γ -rays are found to be strongly beamed (Fan et al. 2014a; Hovatta et al. 2009; Savolainen et al. 2010; Ackermann et al. 2011; Giroletti et al. 2012; Giovannini et al. 2014).

Variability is one of the typical observation properties of blazars, which show variabilities at almost the whole electromagnetic wavebands (Ackermann et al. 2012 and reference therein). The variations have been found to be over time scales from less than one hour to as long as years Fan (2005), who divided the time scales into three classes: micro-variability (intra-day variability, or IDV) with time scale, ΔT being less than one day, short-term variation (STV) with ΔT being one day to several months, and long-term variation (LTV) with ΔT being longer than one year. From observations, we can see that the short-term variations are non-periodic while the long-term variation in some cases is quasi-periodic as discussed in literatures (Jurkevich 1971; Sillanpää et al. 1988; Fan et al. 1998a, 2002; Ciaramella et al. 2004; Wu et al. 2006; Ciprini et al. 2007; Fan et al. 2007; Valtonen et al. 2008; Rani et al. 2010; Wiita 2011; Qian & Tao 2004; Gupta 2014; Gaur et al. 2015a,b).

Photometric monitoring programme can also provide opportunity for people to investigate possible variability periods. The long-term variability period has been explained by various mechanisms (Ciaramella et al. 2004), such as shocks in jets, changes in the direction of forward beaming, and precession in a binary black-hole system (Sillanpää et al. 1988; Camenzind & Krockenberger 1992; Rieger & Mannheim 2000; Valtonen et al. 2008). It has been claimed that the possible periodicity in the historical light curves also shows helical trajectories in their VLBI radio components (Villata & Raiteri 1999).

BL Lac AO 0235+164 ($02^h38^m38.9^s + 16^d36^m59^s$ (2000.0), $A_R = 0.173$), located at $z_{EM} = 0.94$ (Cohen et al. 1987), is a well studied object. Its earlier optical spectroscopy revealed two absorption line systems, one at $z_{abs} = 0.524$ and the other one at $z_{abs} = 0.852$ discovered by Burbidge et al. (1976) and by Rieke et al. (1976). It is observed from radio to X-ray bands, and even high energetic γ -ray regions. It shows variability timescales from less than one hour to several years (Webb et al. 2000; Romero et al. 1997, 2000; Fan et al. 2002; Peng & de Bruyn 2004; Hagen-Thorn et al. 2008; Ackermann et al. 2012; Wang 2014; Vol'vach et al. 2015). Its historic optical variation is over 5 magnitudes (Rieke et al. 1976; Webb et al. 2000). In our previous paper, variations in the UBVRI bands are $\Delta U = 4.26$, $\Delta B = 5.47$, $\Delta V = 4.74$, $\Delta R = 4.18$, and $\Delta I = 3.85$ mag. (Fan & Lin 2000).

AO 0235+164 has been the target of several WEBT campaigns (Raiteri et al. 2001; ?, 2005, 2008) and one of the GASP sources (Ackermann et al. 2012). It shows a bluer-when-brighter (BWB) trend when it was in bright flares but no clear BWB trend when it was in faint low amplitude flares as claimed by Sasada et al. (2011) (see also Sasada 2012). It

is also a highly polarized BL Lac object. Sasada (2012) found that the polarization varied from 0 to $\sim 30\%$, and the high polarizations correspond to bright outbursts. Polarization variation between 35% and 13% on nightly time scale is recently reported (Larionov et al. 2015). The highest degree of polarization, $P = 43.9\%$ was reported by Impey et al. (1982), and the polarization value was renewed to be $P \sim 50\%$ in the paper (Hagen-Thorn et al. 2008). Raiteri et al. (2001) analyzed about 25 years of observational data in optical and radio bands during the period from 1975 to 2000, and found a quasi-periodicity of the main radio (and optical) outbursts on a 5.7-year time scale. A period of 5.87 ± 1.3 years was found in our previous work based on 16 years of optical observations (Fan et al. 2002), but 5.8 ± 0.3 years (based on 14.5 GHz light curve), 5.7 ± 0.3 years (based on 8.0 GHz light curve), and 10.0 ± 1.3 years (based on 4.8 GHz light curve) are found in its radio bands (Fan et al. 2007). It perhaps suggests existence of a binary black hole system at its center (Romero et al. 2003; Ostorero et al. 2004). Very recent analysis based on the long term multiwavelength observations implies that AO 0235+164 hosts a close binary supermassive black holes with similar masses of the order of $10^{10} M_{\odot}$ (Vol'vach et al. 2015). Variabilities on time scales of ~ 17 days, ~ 162 days, and ~ 275 days were also reported (Rani et al. 2009). Short variability time scale is from 0.31 hrs in polarization variability to 6.15 hrs in V band photometry (Hagen-Thorn et al. 2008) while extreme intra-night variability with amplitudes of $\sim 100\%$ over time scales of 24 hours, and changes of 0.5 magnitudes in both R and V bands within a single night, and variations of 1.2 magnitudes from night to night were detected (Romero et al. 2000). AO 0235+164 is one of the objects in our monitoring programme at Abastumani Observatory, Georgia (Kurtanidze et al. 2007; Nikolashvili & Kurtanidze 2007; Fan et al. 2004, 2014b).

The paper is arranged as follows. In section 2, we describe the observations and the data reduction; in section 3, give analysis results; and in section 4, give discussions and conclusions.

2. Observations

2.1. Optical Observations and Data Reduction

Abastumani Observatory is located at the top of the Mountain Kanobili in the South-Western part of Georgia. Mt. Kanobili is about 1,700 meters above the sea level with a latitude of $41^{\circ}.8051$ and a longitude of $42^{\circ}.8254$ respectively. The weather and seeing conditions are excellent (about 1/3 clear nights per year with seeing ≤ 1 arcsec). The mean values of the night sky brightness are $B = 22.0$, $V = 21.2$, $R = 20.6$, and $I = 19.8$ magnitude.

All our observations were made using a 70 cm meniscus telescope ($f/3$), to which a Peltier cooled ST-6 CCD imaging camera was attached to the Newtonian focus from March 1997 to Sept 2006. Post October 2006 an Apogee Ap6E CCD camera (1024×1024 , 24×24 micron, quantum efficiency are 0.40 and 0.72 at 400 nm and 560 nm, respectively) was attached to a primary focus. The readout, digitizing, downloading time is 1 sec. We used only the central portion 350×350 square pixels (15×15 square arcmin), while entire FOV is 40×40 square arcmin.

All our observations are made using the filter R_C passband (Kurtanidze & Nikolashvili 1999). Our exposure times are 60 to 300 seconds. The processing of image frames (bias correction, flat fielding, cosmic rays removal, etc.) and the photometry of the calibrated image frames are carried out by the standard routines in Daophot II. For Daophot II, the aperture was of a fixed diameter size of 10 arc seconds. See our previous work (Fan et al. 2014b) for details.

For the comparison stars (S_i , $i = 1, 2, 3, N$) and the target (O), we calculate the differential magnitude, $O - S_i$, and the corresponding uncertainties σ_{O-S_i} . For the comparison stars, we also calculate the differential magnitudes (Δm_{ij}), and the corresponding uncertainties ($\sigma_{\Delta m_{ij}}$) of any two comparison stars in the field. Here $\Delta m_{ij} = m_i - m_j$, m_i and m_j are the magnitudes of comparison stars, S_i and S_j respectively. For the uncertainty calculation, we take into account CCD chip parameters, sky background, source and comparison star counts (See Kurtanidze & Nikolashvili, 2002). Finally, we choose the two stars which show the minimum deviation as our comparison stars, S_1 and S_2 . The magnitude of the object can be determined using S_1 (or S_2), the corresponding uncertainty of σ_{O-S_1} (or σ_{O-S_2}) is taken as the uncertainty of the observation.

Romero et al. (1999) (see also Cellone et al. 2000 and Fan et al. 2001) introduced a variability parameter, $C_i = \frac{\sigma_{(O-S_i)}}{\sigma_{(S_1-S_2)}}$, $i = 1$ and 2 , to check the reality of a variability. Here, $\sigma_{(O-S_i)}$ is the deviation of the difference of the target object and the comparison star, $\sigma_{(S_1-S_2)}$ is the deviation of the two comparison stars. If $C (= \frac{C_1+C_2}{2})$, the average value of C_1 and C_2 , is greater than 2.576, then the nominal confidence level of a variability detection is greater than 99%.

In 2012, Gaur et al. adopted the standard F -test discussed by de Diego (2010). The F -test is a properly distributed statistics. For two samples, one is the object differential light curve measurements, the other is differential light curve measurements of comparison star. If their variances are S_O^2 and S_C^2 respectively, then $F = \frac{S_O^2}{S_C^2}$.

For observations, the number of degrees of freedom for each sample, ν_O and ν_C are the same and equal to the number of measurements, N , minus 1 ($\nu = N-1$). To investigate the

reality of variation in a source, we compare the F value with the critical value, $F_{C(\nu_O, \nu_C)}(\alpha)$, where α is the significance level set for the test. The smaller the α , the more improbable that the result is produced by chance. If F is greater than the critical value, the null hypothesis (no variability) is discarded. We have performed F-tests at two significance levels (1% and 0.1%) which correspond to 2.6σ and 3σ detections respectively (See de Diego 2010 and Gaur et al. 2012 for details).

In our previous paper, we proposed that a variability can be taken as real if the variability is 3 times greater than the deviation, namely $\Delta m_{12} = m_1 - m_2 \geq 3\sqrt{\sigma_1^2 + \sigma_2^2}$, where σ_1 and σ_2 are the uncertainties corresponding to m_1 and m_2 , the corresponding time interval is adopted as the time scale $\Delta T = t_{m2} - t_{m1}$ (Fan et al. 2009). The time scale can also be expressed as $\Delta T_v = \Delta S/(dS/dt)$, here S is the flux density.

The variability amplitude can be expressed as (Heidt & Wagner 1996):

$$A = 100 \times \sqrt{(m_{max} - m_{min})^2 - 2\sigma^2} (\%), \quad (1)$$

here m_{max} and m_{min} are the maximum and minimum magnitudes in the light curves, σ is the averaged measurement error of the observing run.

In this paper, the optical R -band observations were carried out from Nov. 2006 to Dec. 2012. The data obtained in present paper have used the standard stars 8, 9, 10, and 11 (González-Pérez et al. 2001). From our calculations, the comparison stars 9 and 11 are satisfied for the minimum deviation, $\sigma_{9-11} = 0.008$, and are used as comparison stars in our photometry determinations of AO 0235 + 164. The R -band observations are listed in Table 3, the light curve for AO 0235 + 164 is shown in Fig. 1.

2.2. Radio Observations and Data Reduction

The flux density monitoring observations of AO 0235+164 were carried out at more or less a monthly sampling rate at 4.8 GHz from Dec. 2006 to Nov. 2009 with the Urumqi 25-m radio telescope, with the central frequency of 4.8 GHz and bandwidth of 600 MHz. The typical system temperature is 24 K in clear weather, and the antenna sensitivity is ~ 0.12 K/Jy.

The observations were performed in cross-scans mode, consisting of 8 sub-scans in azimuth and elevation over the source position. After initial calibration of the raw data, the intensity profile of each sub-scan was fitted with a Gaussian function after subtracting a baseline, then the fitted scans were averaged in azimuth and elevation, respectively. After this correction for residual pointing errors was obtained and the elevation and azimuth

scans were averaged together. In the next step an antenna gain elevation correction was applied, including the correction for air mass. The antenna gain-elevation correction was derived from frequent observations of secondary calibrators observed during each observing run. These calibrators were further used to correct the data for systematic time-dependent effects. Finally, the raw amplitudes were converted to the absolute flux density using the average scale of the primary calibrators, e.g. 3C48, 3C286 (Baars et al. 1977; Ott et al. 1994). The radio observations are listed in Table 4 and shown in Fig. 2.

3. Results and Analysis

3.1. Optical Results

From Table 3 (or light curve in Fig. 1), we can see that AO 0235+164 is extreme variable. It shows a variation of $\Delta R \sim 4.88$ mag from $R = 14.19$ to $R = 19.0695$ mag in the whole observing period. The light curve shows 6 clear peaks at JD 2454151 ($R = 14.3738$ mag), JD 2454754 ($R = 14.3258$ mag), JD 2455093 ($R = 16.8380$ mag), JD 2455488 ($R = 17.7453$ mag), JD 2455907 ($R = 17.2259$ mag), and JD 2456207 ($R = 17.7349$ mag). The first two peaks occurred at an interval of 603 days, and then the sources declined to $R = 19.0695$ at 2455479, next it brightened again to $R = 17.7453$ mag in 9 days, and finally to $R = 17.2259$ mag at JD 2455907.

From the works (Heidt & Wagner 1996; Fan et al. 2009), we can discuss variability amplitude, A , and variability time scale (ΔT). During a 5-day observing period of JD 2454120 to JD 2454125, its brightness changed from $\langle R \rangle = 16.0370 \pm 0.0659$ at JD 2454120 to $\langle R \rangle = 16.1697 \pm 0.0414$ at JD 2454122, and to $\langle R \rangle = 15.6913 \pm 0.0660$ at JD 2454124, and afterwards declined to $\langle R \rangle = 16.0427 \pm 0.0430$ at JD 2454125. A brightening of $A = 73.35\%$ in two days (from JD 2454122 to JD 2454124) followed by a dimming of $A = 62.44\%$ within one day, the corresponding variability parameter is $C = C_1 + C_2)/2 = (25.43 + 25.21)/2 = 25.32$. The light curve is shown in Fig. 3(a). The variation, and the corresponding C values and the F values are listed in Table 1. At JD 2454120, its brightness decreased from $R = 15.932$ to $R = 16.188$ within 42 min, the corresponding variability amplitude, time scale, and variability parameter are $A = 25.0\%$, $\Delta T_v = 73.5$ min, and $C = 9.58$ (see Fig. 4(a)). The time scale, variability, and the corresponding C values and the F values are listed in Table 2.

During the period of JD 2454140 to JD 2454151, it decreased from $R = 15.3382$ to 15.8608 within 2 days, corresponding to $\Delta R \sim 0.528$ mag over 2 days and kept this state for 4 days, then brightened again to 15.4587 within 2 days and finally to 14.3738 in the

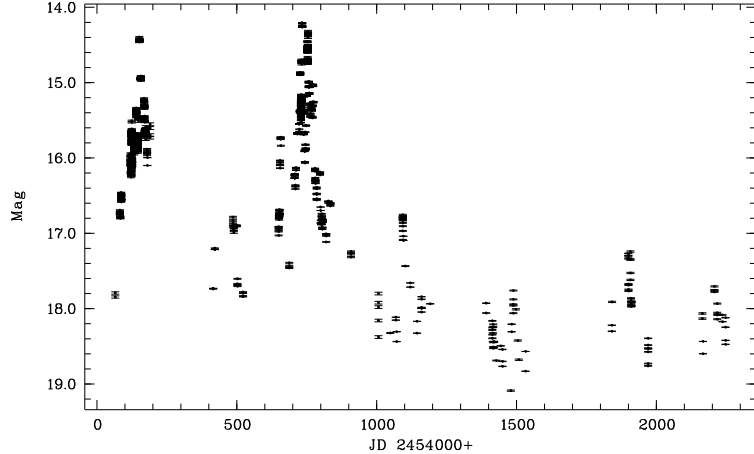


Fig. 1.— Optical R photometry results of 0235+164 during the observing period of 2006 to 2012.

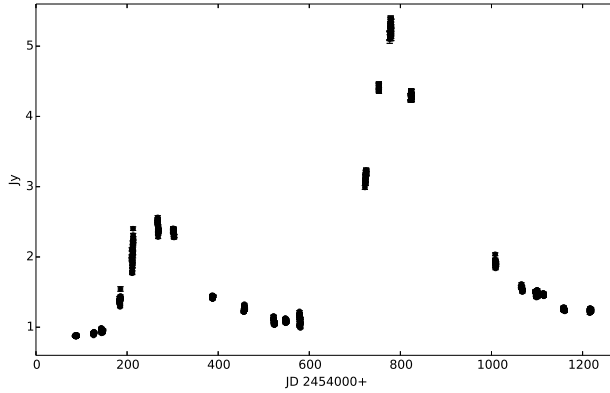


Fig. 2.— Radio light curve of AO 0235+164 during 2006 to 2009.

Table 1: Results of short-term variability (STV) of AO 0235+164

Observation Time	N	C-Test C_1, C_2, C	F $F_1, F_2, F_c(0.99), F_c(0.999)$	Variable
JD2454120-2454125	147	25.43 , 25.21 , 25.32	645.10 , 632.28 , 1.48 , 1.68	V
JD2454140-2454152	283	46.21 , 46.37 , 46.29	2132.98 , 2137.65 , 1.33 , 1.45	V
JD2454168-2454190	76	19.96 , 19.88 , 19.92	397.26 , 393.82 , 1.72 , 2.06	V
JD2454649-2454657	34	75.45 , 75.47 , 75.46	5670.62 , 5657.99 , 2.28 , 3.04	V
JD2454706-2454785	342	49.98 , 49.90 , 49.94	2475.78 , 2476.47 , 1.27 , 1.40	V
JD2455068-2455120	23	95.14 , 95.36 , 95.25	9032.52 , 9029.95 , 2.79 , 3.99	V

Table 2: Results of intra-day variability (IDV) of AO 0235+164

Observation Time	N	C-Test C_1, C_2, C	F $F_1, F_2, F_c(0.99), F_c(0.999)$	Variable	A(%)	ΔT (min.)
JD2454120	20	9.30 , 9.85 , 9.58	86.50 , 96.85 , 3.13 , 4.69	V	25.0	73.5
JD2454142	52	5.33 , 5.33 , 5.33	28.30 , 23.85 , 1.94 , 2.42	V	10.0	252
JD2454730	45	5.15 , 4.67 , 4.91	26.56 , 21.48 , 2.04 , 2.60	V	10.87	144.5
JD2454752	36	5.09 , 4.91 , 5.00	25.39 , 24.00 , 2.23 , 2.93	V	10.74	499

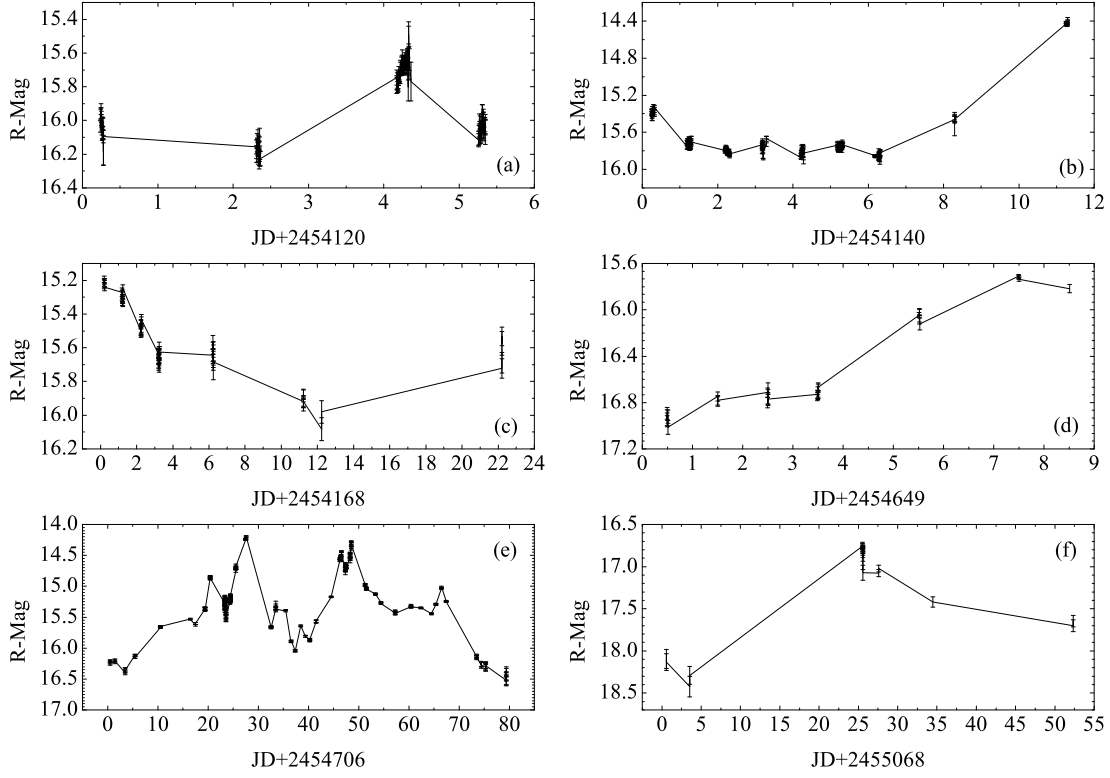


Fig. 3.— Short-term variability of AO 0235+164. (a) during JD 2454120 to JD 2454125, (b) during JD 2454140 to JD 2454151, (c) during JD 2454168 to JD 2454190, (d) during JD 2454649 to JD 2454657, (e) during JD 2454706 to JD 2454785, and (f) period of JD 2455068 and 2455120.

following 3 days, suggesting a brightening of $\Delta R \sim 1.537$ mag within 5 days (see Table 1 and Fig. 3(b)). The corresponding variability parameter during this period is $C = 17.4$. At JD 2454142, there is a variability with $A = 10\%$ within 152 min (corresponding to a time scale of $\Delta T_v = 252$ min.), see Table 2 and Fig. 4(b)).

During the period of JD 2454168 to JD 2454190, it decreased from $R = 15.2222$ to 15.7091 within 3 days, and kept this state for 3 days, and then it decreased to $R = 16.0837$ (JD 2454180) within 4 days, corresponding to $\Delta R \sim 0.8173$ mag over 12 days. After that it increased to $R = 15.5333$ at JD 2454190, corresponding to a variation of $\Delta R \sim 0.4204$ mag over 10 days. See Table 1 and Fig. 3(c).

During the period of JD 2454649 to JD 2454657, its brightness increased from $R = 17.0138$ (JD 2454649) to $R = 15.7101$ (JD 2454656), corresponding to a variability of $\Delta R \sim 1.3037$ mag over 7 days. See Table 1 and Fig. 3(d).

During the period of JD 2454706 to JD 2454785, the light curve shows three peaks with $R = 14.19$, 14.2979 , and 15.0057 with an interval between any close on two peaks being about 20 days. From JD 2454707 to JD 2454733, its brightness increased, and post JD 2454754, it decreased with two peaks. See Table 1 and Fig. 3(e).

At JD 2454730, we have 46 sets of data as shown in Fig. 4(c), it shows a variation of $\Delta R \sim -0.11$ mag over 113 min. corresponding to $A = 10.87\%$, $\Delta T_v = 144.5$ min, and $C = 5.1$. At JD 2454752, we have 37 sets of data as shown in Fig. 4(d), it shows a variation of $\Delta R \sim 0.15$ mag within 5.83 hrs corresponding to $A = 10.74\%$ and $\Delta t_v = 499$ min. See Table 2

During the period of JD 2454797 to JD 22454800, its brightness dimmed from $R = 16.1707$ to $R = 16.8523$ corresponding to a $\Delta R = 0.6816$ mag over 3 days. In the period of JD 2455068 and 2455120, it dimmed from $R = 18.0956$ to 18.4222 over 3 days, then it brightened to $R = 16.7378$ within 22 days, and then dimmed to $R = 17.646$ in 17 days. See Table 1 and Fig. 3(f).

3.2. Radio Results

At radio band, we made observations during the period of Dec. 2006 to Nov. 2009, the results are listed in Table 4 and shown in Fig. 2. We can see clearly that during the optical observing period, radio band also shows two peaks: peak 1 is at JD 2454267 with $f_{\text{peak}} \sim 2.56$ Jy and peak 2 is at JD 2454779 with $f_{\text{peak}} \sim 5.32$ Jy. The corresponding interval is about 510 days. From peak 2, we can see clearly that it brightened from $f \sim 1.12$ Jy to $f \sim 5.32$ Jy in 188 days and then dimmed to $f \sim 1.24$ Jy in 439 days showing a rapid rising and a slow decreasing.

3.3. Discrete Correlation Function (DCF) Analysis

Our long-term monitoring programs of AO 0235+164 were carried out with the 70-cm telescope at Abstumani Observatory, Georgia and the 25-m radio telescope at Xinjiang Astronomical Observatory, Chinese Academy of Sciences. We obtained a coverage of 12 years of optical data and 3 years of radio data. We hereby investigate whether there is any correlation and/or time delay between optical and radio bands. To study this, we adopted the discrete correlation function (DCF) method to the radio and optical data. The DCF method, which was described in details (Edelson & Krolik 1988) (also see Fan et al. 1998b), is intended for analysis of the correlation of two data sets. This method can indicate the correlation of two variable temporal series with a time lag, τ .

Firstly, the set of unbinned correlation (UDCF) between data points in the radio and optical data streams a (for the optical data) and b (for the radio data) is calculated by

$$UDCF_{ij} = \frac{(a_i - \bar{a}) \times (b_j - \bar{b})}{\sqrt{\sigma_a^2 \times \sigma_b^2}}, \quad (2)$$

where a_i and b_j are points in the data sets, \bar{a} and \bar{b} the averaged values of the data sets, a_i and b_j , and σ_a and σ_b the corresponding standard deviations. Secondly, averaging the points sharing the same time lag by binning the $UDCF_{ij}$ in the suitable sized time-bins in order to get the DCF for each time lag τ :

$$DCF(\tau) = \frac{1}{M} \sum UDCF_{ij}(\tau), \quad (3)$$

where M is the total number of pairs. The standard deviation for each bin is

$$\sigma(\tau) = \frac{1}{M-1} \{ \sum [UDCF_{ij} - DCF(\tau)]^2 \}^{0.5}. \quad (4)$$

When relations (2) to (4) are applied to the optical R flux density, F_R (mJy), (F_R (mJy) = $3.08 \times 10^{6-0.4m_R}$, Mead et al. 1990. $A_R = 0.173$ is adopted for the R magnitude) and the radio data, f_{GHz} (mJy), and only the data carried out during the same observing period are considered, a DCF result is obtained and shown in Fig. 5. For optical and radio variation, a marginal correlation is found with optical variation leading radio variation by 23.2 ± 12.9 days.

3.4. Period Analysis

Now, we have compiled the optical data from literature (also see Fan et al. 2002; Wang 2014), and got an optical light curve covering a time span of 30 years as shown in Fig. 6. It is clear that the light curve is not evenly sampled, which makes periodicity analysis not easy. For the unevenly sampled time series, there are some periodicity analysis methods. Autocorrelation Function (ACF), Structure function (SF), Jurkevich method and Power spectra density (PSD) for instance.

Autocorrelation Function (ACF): ACF is the correlation of a time series with itself at different time. It is a time-domain tool for finding repeating patterns. In statistics, the ACF is the correlation between values of the time series at different times, as a function of the two times or of the time lag.

In the case of the unevenly sampled time series X_{t_i} , $i = 1, 2 \dots N$, the covariance between the time series X_{t_i} and itself with a time lag s is defined as

$$C(s, m) = \frac{\sum_{i=1}^N \sum_{j=1}^N (X_{t_i} - \mu)(X_{t_j} - \mu) \exp[-\frac{(t_i - t_j - s)^2}{2m^2}]}{\sum_{i=1}^N \sum_{j=1}^N \exp[-\frac{(t_i - t_j - s)^2}{2m^2}]}, \quad (5)$$

where μ is the mean of X_{t_i} and m is the width of the gaussian weight function. As the covariance defined above, it can be noted that there are two variances $\sigma(s, m)_1$ and $\sigma(s, m)_2$, and the two variances could be defined as

$$\sigma(s, m)_1 = \left(\frac{\sum_{i=1}^N \sum_{j=1}^N (X_{t_i} - \mu)^2 \exp[-\frac{(t_i - t_j - s)^2}{2m^2}]}{\sum_{i=1}^N \sum_{j=1}^N \exp[-\frac{(t_i - t_j - s)^2}{2m^2}]} \right)^{-\frac{1}{2}}, \quad (6)$$

$$\sigma(s, m)_2 = \left(\frac{\sum_{i=1}^N \sum_{j=1}^N (X_{t_j} - \mu)^2 \exp[-\frac{(t_i - t_j - s)^2}{2m^2}]}{\sum_{i=1}^N \sum_{j=1}^N \exp[-\frac{(t_i - t_j - s)^2}{2m^2}]} \right)^{-\frac{1}{2}}. \quad (7)$$

Then the definition of the autocorrelation of X_{t_i} is

$$R(s, m) = \frac{C(s, m)}{\sigma(s, m)_1 m \sigma(s, m)_2}. \quad (8)$$

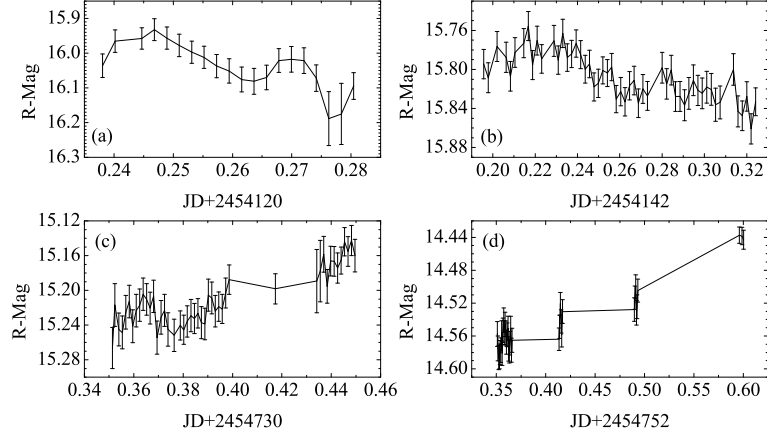


Fig. 4.— Intraday variability of AO 0235+164, (a) at JD 2454120, (b) at JD 2454142, (c) at JD 2454730, and (e) at JD 2454752

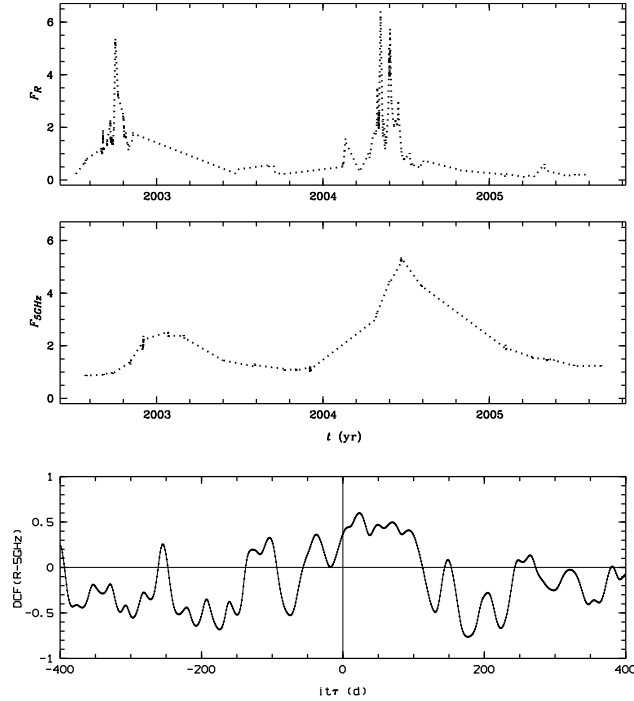


Fig. 5.— Optical and radio light curves and DCF result for optical and radio light curves for AO 0235+164. Top panel is for optical light curve from our observations, middle panel is for radio light curve from our observations, and bottom panel is for the DCF result.

The *ACF* of X_{t_i} is, itself, periodic with the same period. Periodicity analysis results of AO 0235+164 obtained by *ACF* method are shown in the top panel of Fig 7.

Structure Function (SF): Structure function were first considered by (Kolmogorov 1941a,b). The *SF* was discussed in papers (Schulz-Dubois & Rehberg 1981; Emmanoulopoulos et al. 2010). Similar to the *ACF*, the *SF* can also be a tool of periodic analysis.

For the unevenly sampled time series X_{t_i} , the *SF* of X_{t_i} and itself with a time lag s is defined as

$$S(s, m) = \frac{\sum_{i=1}^N \sum_{j=1}^N (X_{t_i}^2 - X_{t_j}^2) \exp\left[-\frac{(t_i-t_j-s)^2}{2m^2}\right]}{\sum_{i=1}^N \sum_{j=1}^N \exp\left[-\frac{(t_i-t_j-s)^2}{2m^2}\right]}. \quad (9)$$

The *SF* of X_{t_i} is, itself, peaked at the time point of period. Periodicity analysis results of AO 0235+164 obtained by *SF* method are also shown in the second panel from the top of Fig 7.

Jurkevich Method (JV): In the case that data are unevenly sampled in time series, as we have done in (Fan et al. 2014b), the Jurkevich method (*JV*) (Jurkevich 1971) and improved power spectral analysis (PSA) will be adopted for the possible periodicities.

The *JV* is based on the expected mean square deviation. The deviation $V_m^2(\tau)$ of a giving period τ for a light curve $X(t_i), i = 1, 2, \dots, N$ would be calculated, as described in (Liu et al. 2011; Fan et al. 2014b). If a frequency $f = 1/\tau$ is equal to the true frequency, then $V_m^2(\tau)$ reaches the minimum. The plot of $V_m^2(f)$ against the f is shown in the third panel from the top of Fig 7.

Power spectra density (PSD): Many attempts of power spectral analysis have been made to investigate the periodicity. An improved technique is the DCDFT+CLEANest (*DCDFT: Date-Compensated Discrete Fourier Transform*), (Ferraz-Mello 1981; Foster 1995), a least-square regression on $\sin(\omega t)$, $\cos(\omega t)$ and constant function. The DCDFT is a powerful method for unevenly spaced data, we adopt it to the light curve following Foster (1995).

In the case of unevenly sampled data, irregular spacing introduces myriad complications into the Fourier transform. It will alter the peak frequency (slightly) and amplitude (greatly), even introduce extremely large false peaks. Following proposal by Foster (1995), we also used a CLEANest analysis to clean false periodicities. The CLEANest algorithm can remove false peaks. Firstly, the strongest single peak and corresponding false components are subtracted from the original spectrum, then the residual spectrum is scanned to determine whether the strongest remaining peak is still statistically significant. If so, then the original data are analyzed to find the pairs of frequencies which best models the data, these 2 peaks

and corresponding false components are subtracted, and the residual spectrum is scanned. By repeating the process, producing CLEANest spectrum, till all statistically significant frequencies are included.

We assume that there are 7 independent frequency components to clean the observation data, the CLEANest spectrum is shown in Fig 7. Only two periods: $P_1 = 8.26$ yr and $P_2 = 0.54$ yr can be found with the threshold that $FAP \geq 3\sigma$.

We also use the first order continuous autoregressive process (CAR1) to estimate the false alarm probability (FAP) of red noise. A CAR1 process Y_t , is a model of red noise, can be given by the stochastic difference function (Brockwell & Davis 2002):

$$Y_t = -\frac{1}{\tau} Y_t dt + dW_t.$$

Here, τ is the timescale of the CAR1 process, and W_t is the Weiner process. The value of τ can be obtained from the light curve (Mudelsee 2002), $\tau = 377_{-17}^{+54}$ days. The simulated FAP curves are also shown in Fig 7. We can find only two possible periods, $P_1 = 8.26$ yr, and $P_2 = 0.54$ yr, which show that threshold $FAP \geq 3\sigma$.

When the methods are adopted to our optical data (Nov, 2006 to Dec. 2012), the analysis results are shown in Fig. 8. From the figure, we can see that there are three signals of QPOs, $P_{1,ACF} = 0.37 \pm 0.03$ yr, $P_{2,ACF} = 0.52 \pm 0.02$ yr and $P_{3,ACF} = 0.77 \pm 0.04$ yr can be derived by using ACF method, three signals of QPOs, $P_{2,SF} = 0.37 \pm 0.03$ yr, $P_{2,SF} = 0.52 \pm 0.02$ yr and $P_{3,SF} = 0.77 \pm 0.04$ yr can be found by using SF method, and three similar signals of QPOs, $P_{1,JV} = 0.39 \pm 0.03$ yr, $P_{2,ACF} = 0.50 \pm 0.02$ yr and $P_{3,ACF} = 0.72 \pm 0.05$ yr can be obtained by using JV method. Based on the above results, there are QPOs but not identical but nearly similar period, their average value gives, $P_{avg} = 0.55 \pm 0.03$ yr. The P_{avg} is consistent with the 0.54 yr period sign.

4. Discussions and Conclusions

Variability is one of the extreme properties of BL Lacertae objects. Variability can be divided into three classes according to their time scales: micro-variability with time scale being less than one day; short-term variability with time scale being a few days to months; long-term variation with time scale being years (Fan 2005). But it is not easy to say whether a variation is real or not. It can be taken as a real variability if the variability shows up in simultaneous multiwavelength observations. Unfortunately, it is not always the case for one to do simultaneous multiwavelength observations, and most of monitoring programs are performed at a certain waveband. Romero et al. (1999) introduced a variability

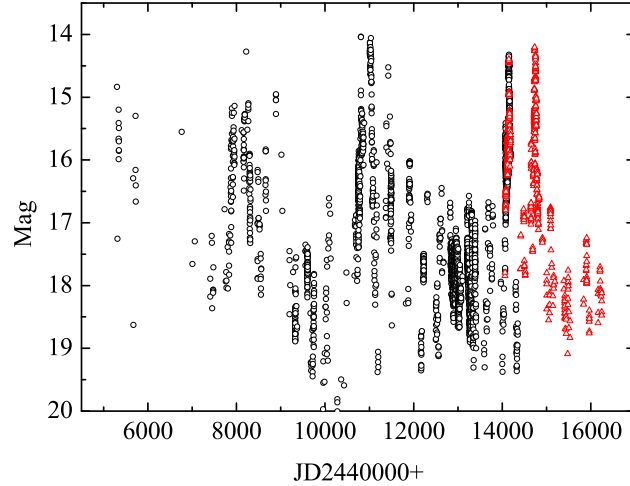


Fig. 6.— Historic light curve of AO 0235+164 during JD 2445300 to JD 2456247. The open circles are from the literatures and the triangles are from our own observations.

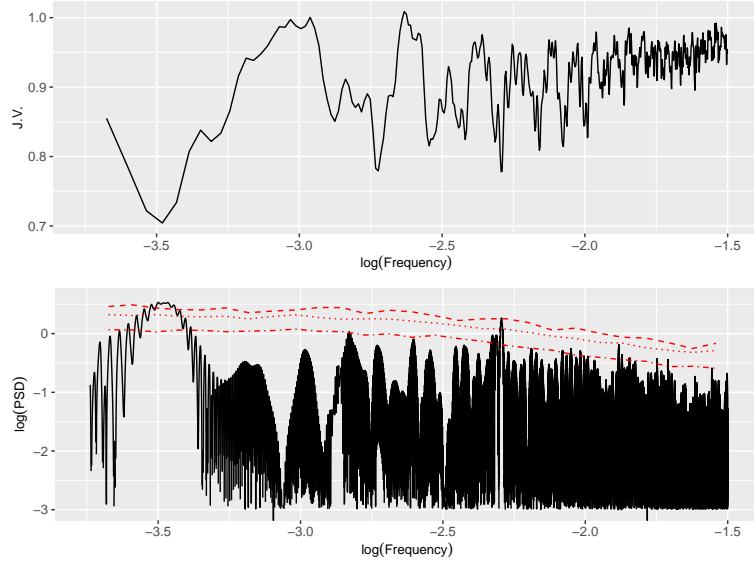


Fig. 7.— Top panel: Periodicity analysis results of AO 0235+164 obtained by Jurkevich method. Bottom panel: results for AO 0235+164 by PSA method. The curves of the false alarm probability by using CAR1 method are also plotted. Two signals, $P_1 = 8.26$ yr, and $P_2 = 0.54$ yr, can be found with the threshold that $FAP \geq 3\sigma$.

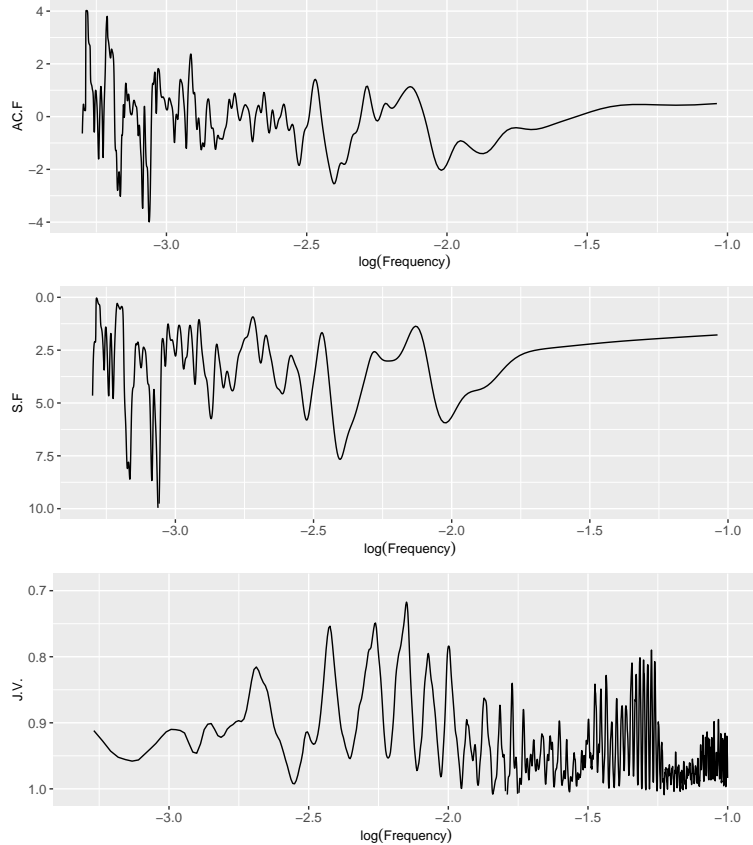


Fig. 8.— Periodicity analysis results of AO 0235+164 based on our own observations and obtained by different methods: Top panel: Three signals of QPOs, $P_{1,ACF} = 0.37 \pm 0.03$ yr, $P_{2,ACF} = 0.52 \pm 0.02$ yr and $P_{3,ACF} = 0.77 \pm 0.04$ yr by *ACF* method; Middle panel: $P_{2,SF} = 0.37 \pm 0.03$ yr, $P_{2,SF} = 0.52 \pm 0.02$ yr and $P_{3,SF} = 0.77 \pm 0.04$ yr by *SF* method; Bottom panel: $P_{1,JV} = 0.39 \pm 0.03$ yr, $P_{2,ACF} = 0.50 \pm 0.02$ yr and $P_{3,ACF} = 0.72 \pm 0.05$ yr by *JV* method.

parameter C , to justify a variation to be strong or not. de Diego (2010) introduced a F -test for the discussion of variability (see also Gaur et al. 2012). Heidt & Wagner (1996) proposed a method to obtain a variability amplitude A . We also proposed that a variation can be taken as a real one if the variability is 3 times greater than the deviation, namely $\Delta m_{12} = m_1 - m_2 \geq 3\sqrt{\sigma_1^2 + \sigma_2^2}$, where σ_1 and σ_2 are the uncertainties corresponding to m_1 and m_2 , the corresponding time interval is adopted as the time scale $\Delta T = t_{m2} - t_{m1}$ (Fan et al. 2009). Time scale is also defined to be $\Delta T_v = \Delta F/(dF/dt)$.

AO 0235 + 164 is one of the well studied objects. Although it was classified as a BL Lac object, the equivalent width (EW) of emission lines varies from one observational epoch to another. It is violently variable in all wavebands from radio through high energetic γ -rays (Ackermann et al. 2012). Its synchrotron peak frequencies obtained by different authors are $\log\nu_p$ (Hz) = 13.29 (Fan et al. 2016), 13.39 (Sambruna et al. 1996), 13.57 (Nieppola et al. 2006), and 13.10 (Abdo et al. 2010a), suggesting it to be a low-synchrotron peaked (LSP) BL Lac. During the 2008 September to 2009 February outburst period, the γ -ray activity is correlated with near infrared/optical flares, but there is no clear correlation between γ -ray and radio emissions (Ackermann et al. 2012).

Intraday radio variabilities were detected in the works (Quirrenbach et al. 1992; Romero et al. 1997; Kraus et al. 1999). Its unusual radio outburst detected at $\lambda = 20\text{cm}$ results in a brightness temperature of $T_B \sim 7 \times 10^{17}\text{K}$ for $\Delta t_{20\text{cm}} \sim 2\text{days}$ (Kraus et al. 1999). Such a high brightness temperature suggests a very large Doppler factor of $\delta \sim 100$. For the source, radio components show superluminal velocities as fast as $\beta \sim 30h^{-1}$ ($h = H/100\text{km Mpc}^{-1}\text{s}^{-1}$) (Abraham et al. 1993; Chu et al. 1996; Jorstad et al. 2001). Let $h \sim 0.67$, $\beta \sim 30h^{-1}$ suggests a $\delta \sim 2\Gamma = 2\beta \sim 90$.

At the optical bands, rapid variability was reported by many authors (Schramm et al. 1994; Heidt & Wagner 1996; Romero et al. 2000; Gaur et al. 2012). Schramm et al. (1994) reported an extreme optical variability of 1.6 mag within 48 hours. Heidt & Wagner (1996) found variation amplitude of 6.33% per day. Romero et al. (2000) reported an intra-night variability with amplitudes of $A \sim 100\%$ over 24 hours, variations of $\Delta m = 0.5$ mag were detected in R and V bands within a single night, and variations up to 1.2 magnitudes occurred from night to night.

In the soft X-ray region, ROSAT detected an increasing by a factor of 1.7 in about 3 days, and a decreasing of a factor of 3.5 in about 13 days (Urry et al. 1996), which suggest doubling time scales of $\Delta T_D = 1.76$ and 3.71 days respectively.

4.1. Variability

For AO 0235+164, its historic variation amplitude is as large as $\Delta m \sim 5.0$ mag (Rieke et al. 1976; Stein et al. 1976; Fan & Lin 2000). In our monitoring period, the light curve shows a variation amplitude of $\Delta R \sim 4.88$ mag and 6 peaks, the 6 peaks show intervals of 1.65, 0.93, 1.08, 1.15, and 0.82 years. The largest variation amplitude in our observations is similar to the historically largest amplitude.

It shows different time scales, a brightness decreasing of $\Delta R = 0.8173$ mag over 12 days (JD 2454168 to JD 2454180), $\Delta R = 0.6816$ mag over 3 days (JD 2454797 to JD 22454800) and 0.3366 mag over 3 days (JD 2455068 and 2455120), $\Delta R = 0.528$ mag over 2 days (JD 2454140-JD 2454142), and $\Delta R = 0.627$ mag ($A = 62.44\%$) over 1 day (JD 2454124 to JD 2454125). A brightness increase of $\Delta R = 0.4204$ mag over 10 days (JD 2454180 to JD 2454190), $\Delta R = 1.3037$ mag over 7 days (JD 2454649 to JD 2454656), $\Delta R = 1.537$ mag within 5 days (JD 2454146 to JD 2454151), and $\Delta R = 0.7367$ mag ($A = 73.35\%$) over 2 days (JD 2454122 to JD 2454124). A variation over 2 days was found in a paper by Sagar et al. (2004), who noticed a dramatic brightness fading of 0.83 mag within 2 days in 1999.

Very rapid variabilities are also detected as listed in Table 2. Our monitoring results show that the shortest time scale is $\Delta T_v = 73.5$ min, which is longer than the time scale of 0.31 hrs detected in the polarization variability in V band (Hagen-Thorn et al. 2008).

4.2. Correlation between Optical and Radio Bands

The optical/radio correlation is investigated for AO 0235 + 164 (see Takalo et al. 1992 and references therein). A positive correlation with a delay of $0 \sim 2$ months from optical to radio was reported in a paper (Clements et al. 1995). From our DCF calculation based on our own optical and radio data, we found that there is a marginal correlation with optical variation leading radio variation by 23.2 ± 12.9 days. Our results are consistent with the time-lag of $0 \sim 2$ months by Clements et al. (1995).

AO 0235 + 164 has a complex feature, it shows absorption and emission lines corresponding to redshifts of 0.542 and 0.851 (Burbidge et al. 1976, Smith et al. 1985), 0.92 (Cohen et al. 1987), and 0.94 (Charles, et al. 1994). AO 0235+164 is one of the candidates for the discussions of microlesing phenomena (see Charles et al. 1994, Webb et al. 2000, Rain et al. 2009, Gaur2012). If the outbursts are due to microlensing, the simplest scenarios predict symmetric outbursts that are frequency independent. In our observations, the source display sharp outbursts in its optical band in 2002 and 2004 while broad and delayed outbursts in the radio band at the end of 2002/beginning of 2003 and in the middle of 2004.

The outbursts in the optical band in 2004 have double peaks while that in the radio band is only one broad peak. The DCF analysis shows that the optical variability leads the radio variability by 23.2 ± 12.9 days. So, the outbursts in the optical and radio bands maybe not caused by the microlensing effect.

4.3. Periods

Periodicity analysis is also interesting in active galactic nuclei (AGNs). It was claimed to show up in 3C 120 (Jurkevich 1971), then a lot of AGNs have been reported to show quasi-periodicity signs in their light curves (Sillanpää et al. 1988; Fan et al. 1998a, 2002, 2007, 2010, 2014b; Ciaramella et al. 2004; Wu et al. 2006; Ciprini et al. 2007; Valtonen et al. 2008; Webb et al. 2000; Rani et al. 2010; Qian & Tao 2004; Gupta 2014; Wang 2014; Bon et al. 2016; Wang & Su 2016). As one of the well studied blazars, AO 0235+164 has been observed and periodicity analyzed in many works (Webb et al. 1988; Smith & Nair 1995; Fan et al. 2002, 2007; Raiteri et al. 2001, 2005, 2007, 2008; Wang 2014).

Using discrete Fourier transform(DFT), Webb et al. (1988) analyzed the optical light curve of AO 0235+164 and found periods of 2.79, 1.53 and 1.29 years, later on they removed a linear trend from the light curve and adopted unequal-interval Fourier transform and CLEAN techniques to its normalized data, and obtained periods of 2.7 and 1.2 years. Smith & Nair (1995) found periods of 2.7 and 3.6 years in the optical band. Raiteri et al.(2001) reported a 5.67 year period in the R optical light curve and 1.8, 2.8 and 3.7 years in radio bands. In our previous papers (Fan et al. 2002, 2007), we found periods of 2.0 years, 2.95 ± 0.15 years and 5.87 ± 1.3 years in the optical light curve, and period of 10.0 ± 1.3 years, 5.7 ± 0.3 years and 5.8 ± 0.3 years at 4.8GHz, 8.0 GHz, and 14.5 GHZ light curves.

Raiteri et al. (2001) claimed a possible quasi-periodic occurrence of the major radio and optical outbursts of AO 0235+164 every 5.7 ± 0.5 years, which result in the WEBT campaign observing the source (Raiteri et al. 2005, 2007). The period analysis based on the historic and the campaign observations suggests that the period for the large outburst is $8 \sim 8.5$ years (Raiteri et al. 2005, 2007, 2008; Gupta et al. 2008). It is clear that the periodicity analysis results depend on the observations, that is why different works give different results.

In this work, we find that two periods $P_1 = 8.26$ yr and $P_2 = 0.54 \sim 0.56$ yr have $FAP \geq 3\sigma$ in the optical light curve. However, the time coverage used to investigate the period is only 30 years. As mentioned by Koen (1990) that estimating (rather than knowing) the variance of the time series can change the $FAPs$ by orders of magnitude. Therefore, the periods should be investigated using more dense observations.

4.4. Conclusions

In this work, we have presented the R optical observations during the period of Nov, 2006 to Dec. 2012 and radio observations light curve during the period of Dec. 2006 to Nov. 2009. Following results are obtained:

1. Largest variation is $\Delta R = 4.88$ mag from our observations.
2. The shortest time scale detected in our monitoring program is $\Delta T_v = 73.5$ min.
3. The optical and radio variation is correlated with optical leading radio by 23.2 ± 12.9 days.

acknowledgements

The work is partially supported by the National Natural Science Foundation of China (NSFC U1531245, U1431112, U11203007, 11403006, 10633010, 11173009), the Innovation Foundation of Guangzhou University (IFGZ), Guangdong Province Universities and Colleges Pearl River Scholar Funded Scheme(GDUPS)(2009), Guangdong Innovation Team for Astrophysics(2014KCXTD014), Yangcheng Scholar Funded Scheme(10A027S), and support for Astrophysics Key Subjects of Guangdong Province and Guangzhou City. The Abastumani team acknowledges financial support of the project FR/639/6-320/12 by the Shota Rustaveli National Science Foundation under contract 31/76.

REFERENCES

- Abdo, A. A., Ackermann, M., Agudo, I., et al., 2010a, ApJ, 716, 30
Abdo, A. A., Ackermann, M., Ajello, M., et al., 2010b, ApJS, 188, 405
Abraham, R.G., Crawford, C.S., Merrifield, M. R., Hutchings, J. B., McHardy, I. M., 1993, ApJ, 415, 101
Ackermann, M., Ajello, M., Allafort, A., et al., 2011, ApJ, 743, 171
Ackermann, M., Ajello, M., Ballet, J., Barbiellini, G., Bastieri, D. et al. 2012, ApJ, 751, 159
Ackermann, M., Ajello, M., Atwood, W., et al., 2015, ApJ, 810, 14A
Agarwal, A., Gupta, A. C., Bachev, R., Strigachev, A., Semkov, E., Wiita, P. J., Böttcher, M., et al. 2015, MNRAS, 451, 3882

- Agarwal, A. & Gupta, A. C. 2015, MNRAS, 450, 541
- Baars, J. W. M., Genzel, R., Pauliny-Toth, I. I. K., Witzel, A., 1977, A&A, 61, 99
- Bon, E., Zucker, S., Netzer, H., Marziani, P., Bon, N., Jovanovic, P., Shapovalova, A. I., Komossa, S., et al. 2016arXiv160604606B
- Brockwell, P. J., & Davis, R. A., 2002, Introduction to Time Series and Forecasting (New York: Springer)
- Burbidge, E. M., Caldwell, R. D., Smith, H. E., Liebert, J. & Spinrad H., 1976, ApJ, 205, L117
- Camenzind, M., & Krockenberger, M. 1992, A&A, 255, 59
- Charles, P. A., Kidger, M. R., Lehto, H. J., Nilsson, K., Sillanpa? a? , A., & Takalo, L. O. 1994, Turku Univ. Obs. Informo, No. 174, 87
- Chu, H. S., Baath, L. B., Rantakyro, F. T., et al. 1996, A&A, 307, 15
- Ciaramella, A., Bongardo, C., Aller, H. D, et al., 2004, A&A, 419, 485
- Ciprini, S., Takalo, L. O., Tosti, G., 2007, A&A, 467, 465
- Clements S.D., Smith, G., Aller, H.D., Aller, M.F., 1995, AJ, 110, 529
- Cohen, R. D., Smith, H. E., Junkkarinen, V. T., et al. 1987, ApJ, 318, 577
- Dai, B.Z., Li, X.H., Liu, Z.M., Zhang, B.K., Na, W. W., Wu, Y. F., Hao, J. M., Xiang, Y., et al., 2009, MNRAS, 392, 1181
- Dai, B.Z., Zeng, W., Jiang, Z. J., Fan, Z. H., Hu, W., Zhang, P. F., et al. 2015, ApJS, 218, 18
- de Diego, J. A. 2010, AJ, 139, 1269
- Dominici, T. P., Abraham, Z., Galo, A. L., 2006, A&A, 460, 665
- Edelson, R. A. & Krolik, J. H., 1988, ApJ, 333, 646
- Emmanoulopoulos, D., McHardy, I. M., Uttley, P., 2010, MNRAS, 404, 931
- Fan, J.H., Xie, G.Z., Pecontal, E., Pecontal, A., Copin, Y., 1998a, ApJ, 507, 173
- Fan, J. H., Adam, G., Xie, G. Z., Cao, S. L., Lin, R. G., Qin, Y. P., Copin, Y., Bai, J. M., et al. 1998b, A&AS, 133, 163

- Fan, J.H., & Lin, R.G., 2000, ApJ, 537, 101
- Fan, J. H., Lin, R. G., Xie, G. Z., et al., 2002, A&A, 381, 1
- Fan, J.H., Kurtanidze, O., Nikolashvili, M.G., et al. 2004, ChJAA, 4, 133
- Fan, J.H., 2005, ChJAA (RAA), 5, 213
- Fan, J.H., Tao, J., Qian, B.C., Gupta, A.C., Liu, Y., 2006, PASJ, 58, 797
- Fan, J.H., Liu, Y., Hua, T. X., et al., 2007, A&A, 462, 547
- Fan, J.H., Peng, Q.S., Tao, J., Qian, B. C., Shen, Z. Q., 2009, AJ, 138, 1428
- Fan, J.H., Liu, Y., Qian, B.C. et al. 2010, RAA, 10, 1100
- Fan, J.H., Liu, Y., Li, Y., Zhang, Q.F., Tao, J., Kurtanidze, O., 2011, JAp&A, 32, 67
- Fan, J. H., Bastieri, D., Yang, J. H., Liu, Y. et al. 2014a, RAA, 14, 1135
- Fan, J. H., Kurtanidze, O., Liu, Y. et al. 2014b, ApJS, 213, 26
- Fan, J. H., Yang, J. H., Liu, Y., Luo, G.Y., Lin, C., Yuan, Y.H., Xiao, H.B., Zhou, A. Y., Hua, T.X., Pei, Z.Y., 2016, ApJS, 226, 20
- Ferraz-Mello, S, 1981, AJ, 86, 619
- Foster, G. 1995, AJ, 109, 1889
- Gaur, H., Gupta, A.C., Bachev, R., Strigachev, A., Semkov, E., Wiita, P.J., Peneva, S., Boeva, S., Slavcheva-Mihova, L, Mihov, B., Latev, G., Pandey, U.S., 2012, MNRAS, 425, 3002C3023
- Gaur, H., Gupta, A.C., Bachev, R., Strigachev, A., Semkov, E., Wiita, P.J., Volvach, A. E., Gu, M. F., Agarwal, A., et al. 2015a, A&A, 582A, 103
- Gaur, H., Gupta, A.C., Bachev, R., Strigachev, A., Semkov, E., Böttcher, M., Wiita, P.J., de Diego, J.A., et al. 2015b, MNRAS, 452, 4263
- Giovannini, G., Liuzzo, E., Boccardi, B., Giroletti, M., 2014, IAUS, 304, 200
- Giroletti, M., Pavlidou, V., Reimer, A., et al., 2012, AdSpR, 49, 1320
- González-Pérez, J.N., Kidger, M. R., & Martin-Luis, F., 2001, AJ 122, 2055

- Graham, M. J., Djorgovski, S. G., Stern, D., Drake, A. J., Mahabal, A. A., Donalek, C., Glikman, E., Larson, S., Christensen, E., 2015, MNRAS, 453, 1562
- Gupta, A.C., Cha, Sang-Mok, Lee, S., et al., 2008, AJ, 136, 2359
- Gupta, A.C., 2014, JApA, 35, 307
- Hagen-Thorn, V. A., Larionov, V. M., Jorstad, S. G., et al. 2008, ApJ, 672, 40
- Heidt, J., & Wagner, S. J. 1996, A&A, 305, 42
- Horne, J., & Baliunas, S. 1986, ApJ, 302, 757
- Hovatta, T., Valtaoja, E., Tornikorski, M., et al., 2009, A&A, 496, 527
- Hu, S. M., Chen, X., Guo, D. F., Jiang, Y. G., Li, K., 2014a, MNRAS, 443, 2940
- Hu, S. M., Chen, X., Guo, D. F., 2014b, JApA, 35, 261
- Impey, C. D., Brand, P. W. J. L. & Tapia, S. 1982, MNRAS, 198, 1
- Jorstad, S. G., Marscher, A. P., Mattox, J. R., et al 2001, ApJS, 134, 181
- Jurkevich, I., 1971, Ap&SS, 13, 154
- Koen, C., 1999, MNRAS, 309, 769
- Kolmogorov, A. 1941, Akademiia Nauk SSSR Doklady, 30, 301
- Kolmogorov, A. N. 1941, Akademiia Nauk SSSR Doklady, 32, 16
- Kraus, A., Quirrenbach,A., Lobanov, A.P. et al. 1999, A&A, 344, 807
- Kurtanidze, O. M., Nikolashvili, M. G, 1999, Blazar Monitoring towards the Third Millennium, Proceedings of the OJ-94 Annual Meeting 1999, held in Torino, Italy, May 19-21, 1999, Eds.: C.M. Raiteri, M. Villata, and L.O. Takalo, Osservatorio Astronomico di Torino, Pino Torinese, Italy, p. 25-28
- Kurtanidze, O., Nikolashvili, M., Kimeridze, G. N., Sigua, L. A., Kapanadze, B. Z., 2007, IAUS, 238, 399
- Kurtanidze, O. M., Tetradze, S. D., Richter, G. M., Nikolashvili, M. G., Kimeridze, G. N., Sigua, L. A., 2009, ASPC408, 266
- Larionov, V.M., Borman, G. A., Jorstad, S. G. 2015, ATel #6414

- Liu, Y., Fan, J. H., Wang, H. G., & Deng, G. G., 2011, JApA, 32, 79
- Li, H. Z., Jiang, Y. G., Guo, D. F., Chen, X., Yi, T. F, 2016, PASP, 128g4101
- Marchesini, E. J., Andruchow, I., Cellone, S. A., Combi, J. A., Zibecchi, L., Mart, J., Romero, G. E., Muoz-Arjonilla, A. J., et al. 2016, A&A, 591A, 21
- Mead, A. R. G., Ballard, K. R., Brand, P. W. J. L., Hough, J. H., Brindle, C., Bailey, J. A., 1990, A&AS, 83, 183
- Mudelsee, M., 2002, CG, 28, 69
- Nikolashvili, M., & Kurtanidze, O., 2007, IAUS, 238, 419
- Nieppola, E., Tornikoski, M., & Valtaoja, E. 2006, A&A, 445, 441
- Nolan, P. L., Abdo, A. A., Ackermann, M., et al. 2012, ApJS, 199, 31
- Ostorero, L., Villata, M., Raiteri, C. M. 2004, A&A, 419, 913
- Ott, M., Witzel, A., Quirrenbach, A., Krichbaum, T. P., Standke, K. J., Schalinski, C. J., Hummel, C. A., 1994, A&A, 284, 331
- Padovani, P., & Giommi, P., 1995, ApJ, 444, 567
- Peng, B. & de Bruyn, A. G., 2004, ApJ, 610, 151
- Qian, B.C., & Tao, J., 2004, PASP, 116, 161
- Quirrenbach A., Witzel A, Krichbaum T.P., et al., 1992, A&A, 258, 279
- Raiteri, C. M., Villata, M., Aller, H. D., et al. 2001, A&A, 377, 396
- Raiteri, C. M., Villata, M., Kadler, M., et al. 2006, A&A, 459, 731
- Raiteri, C. M., Villata, M., Capetti, A., et al. 2007, A&A, 464, 871
- Raiteri, C. M., Villata, M., Larionov, V. M., et al. 2008, A&A, 480, 339
- Raiteri, C. M., Villata, M., D'Ammando, F., et al. 2013, MNRAS, 436, 1530,
- Rani, B., Wiita, P., Gupta, A. C., 2009, ApJ, 696, 2170
- Rani, B., Gupta, A. C., Joshi, U. C., Ganesh, S., Wiita, P. J., 2010, ApJ, 719, 153

- Rieke, G. H., Grasdalen, G. L., Kinman, T. D., Hintzen, P., Wills, B. J., Wills, D., 1976, *Nat.*, 260, 754
- Rieger, F.M., & Mannheim, K. 2000, *A&A*, 359, 948
- Romero, G. E., Combi, J. A., Benaglia, P., et al., 1997, *A&A*, 326, 77
- Romero, G. E., Cellone, S. A., Combi, J. A., 1999, *A&AS*, 135, 477
- Romero, G. E., Cellone, S. A., Combi, J. A., 2000, *A&A*, 360L, 47
- Romero, G. E., Fan, J. H., Nuza, S. E. 2003, *ChJAA*, 3, 513
- Sagar, R., Stalin, C.S., Gopal-Krishna, Wiita, P.J., 2004, *MNRAS*, 348, 176
- Sambruna, R. M., Maraschi, L., Urry, C. M., 1996, *ApJ*, 463, 444
- Sasada, M., 2012, *Journal of Physics: Conference Series*, Volume 355, Issue 1, id. 012023
- Sasada, M., Uemura, M., Fukazawa, Y., Kawabata, K. S., Ikejiri, Y., Itoh, R. et al. 2011, *PASJ*, 63, 489
- Savolainen, T., Homan, D. C., Hovatta, T., et al., 2010, *A&A*, 512A, 24
- Scargle, J. 1982, *ApJ*, 263, 835
- Schramm K.-J., Bogaest U., Kuhl D., et al., 1994, *A&AS* 106, 349
- Schulz-Dubois, E. O., & Rehberg, I. 1981, *Applied Physics*, 24, 323
- Sillanpää, A., Haarala, S., Valtonen, M. J., Sundelius, B., Byrd, G. G., 1988, *ApJ*, 325, 628.
- Smith, A. G. & Nair, A.D., 1995, *PASP*, 107, 863
- Smith, P. S., Balonek, T. J., Heckert, P. A., Elston, R., & Schmidt, G. D. 1985, *AJ*, 90, 1184
- Stein, W. A., Odell, S. L., Strittmatter, P. A., 1976, *ARA&A*, 14, 173
- Takalo, L.O., Sillanpää, A., Nilsson, K., Kidger, M., de Diego, J. A., Pirola, V., 1992, *A&AS*, 94, 37
- Taris, F., Andrei, A., Roland, J., Klotz, A., Vachier, F., Souchay, J., 2016, *A&A*, 587A, 112
- Urry, C. M. & Padovani, P., 1995, *PASP*, 107, 803
- Urry, C.M., Sambruna, R. M., Worrall, D.M., et al. 1996, *ApJ*, 463, 424

- Valtaoja, L., Sillanpaa, A., Valtaoja, E., Shakhovskoi, N. M., & Efimov, I. S. 1991, AJ, 101, 78
- Valtonen, M., Kidger, M., Lehto, H., Poyner, G., 2008, A&A, 477, 407
- Villata, M., & Raiteri C. M. 1999, A&A, 347, 30
- Villata, M., Raiteri, C. M., Kurtanidze, O. M., Nikolashvili, M. G., Ibrahimov, M. A., Papadakis, I. E., Tsinganos, K., Sadakane, K., et al., 2002, A&A, 390, 407
- Vol'vach, A. E., Larionov, M. G., Vol'vach, L. N., Lähteenmäki, A., Tornikoski, M., Aller, M. F., Aller, H. D., Sasada, M., 2015, Astron. Rep., 59, 145
- Wang, H. T., 2014, Ap&SS, 351, 281
- Wang, H. T., & Su, Y. P., 2016, NewA, 45, 32
- Webb, J. R. Smith, A. G., Leacock, R. J., Fitzgibbons, G. L., Gombola, P. P., Shepherd, D. W. 1988, AJ, 95, 374
- Webb, J. R., Howard, E., Bentez, E., Balonek, T., et al., 2000, AJ, 120, 41
- Wiita, P. J., 2011, JAp&A, 32, 147
- Wu, J. H., Zhou, X., Wu, X. B., et al., 2006, AJ, 132, 1256
- Wu, X.B., Liu, F.K., Kong, M.Z., Wang, R., Han, J.L, 2011, JApA, 32, 209
- Zhang, B. K., Wang, S., Zhao, X. Y., Dai, B. Z., Zha, M., 2013, MNRAS, 428, 3630

Table 3. Observational data for AO 0235 + 164

JD (1)	R-Mag. (2)	σ (3)
2454065.44811	17.8296	0.0561
2454065.45163	17.7653	0.1019
2454082.33861	16.7107	0.0247
2454082.34072	16.6765	0.0254
2454082.34281	16.6997	0.025
2454082.34492	16.728	0.0261
2454082.34703	16.7373	0.0255
2454082.34912	16.7274	0.0248
2454082.35123	16.7347	0.0259
2454082.35333	16.7054	0.0251
2454083.34441	16.7657	0.0292
2454083.34861	16.7624	0.0318
2454083.35281	16.7825	0.0327
2454083.35492	16.7867	0.0332
2454086.36082	16.5338	0.0238
2454086.36293	16.5452	0.0254
2454086.36565	16.5645	0.0265
2454086.36774	16.5416	0.0252
2454086.36985	16.5401	0.0258
2454086.37196	16.545	0.0257
2454086.37405	16.5555	0.0264
2454086.37616	16.5345	0.0266
2454086.37828	16.5696	0.0272
2454086.38248	16.5336	0.0263
2454086.38458	16.4911	0.0275
2454086.38668	16.5367	0.0282
2454086.38879	16.519	0.0257
2454086.39089	16.4646	0.0243
2454086.39299	16.4902	0.0264
2454086.39509	16.5014	0.0278
2454086.39720	16.499	0.0269
2454086.39929	16.4631	0.027
2454086.40140	16.4843	0.0263
2454086.40351	16.4947	0.0266
2454086.40560	16.541	0.0296
2454086.41657	16.5514	0.0314
2454086.41868	16.5336	0.0313
2454086.42078	16.528	0.039
2454086.42288	16.5082	0.0426
2454086.42500	16.4615	0.0456
2454086.42710	16.4541	0.0324
2454086.42920	16.4883	0.0309
2454086.43131	16.4449	0.0301
2454086.43340	16.466	0.0318
2454086.43551	16.488	0.0326

Table 3—Continued

JD (1)	R-Mag. (2)	σ (3)
2454120.23807	16.0361	0.0337
2454120.24017	15.9652	0.0325
2454120.24471	15.9579	0.0308
2454120.24682	15.932	0.0316
2454120.24891	15.9568	0.0318
2454120.25102	15.9774	0.0323
2454120.25312	15.9971	0.032
2454120.25522	16.0121	0.0318
2454120.25733	16.0373	0.0336
2454120.25943	16.0512	0.0351
2454120.26154	16.0759	0.036
2454120.26363	16.081	0.0371
2454120.26574	16.0701	0.0356
2454120.26784	16.0215	0.0342
2454120.26994	16.0177	0.0367
2454120.27205	16.0214	0.037
2454120.27414	16.0716	0.0381
2454120.27625	16.1884	0.0776
2454120.27836	16.175	0.0881
2454120.28045	16.0948	0.0384
2454122.30978	16.1563	0.041
2454122.31189	16.187	0.0386
2454122.31399	16.2093	0.0409
2454122.31609	16.205	0.0425
2454122.31819	16.1533	0.0402
2454122.32030	16.1187	0.0412
2454122.32240	16.1433	0.0397
2454122.32450	16.1698	0.0412
2454122.32661	16.1507	0.0409
2454122.32870	16.1238	0.0382
2454122.33081	16.0947	0.0388
2454122.33292	16.1468	0.0372
2454122.33501	16.2157	0.0436
2454122.33712	16.1678	0.0404
2454122.33922	16.133	0.0408
2454122.34132	16.1629	0.0413
2454122.34343	16.1715	0.0415
2454122.34553	16.2209	0.0476
2454122.34763	16.2404	0.0466
2454122.34973	16.1373	0.0392
2454122.35185	16.0849	0.0379
2454122.35395	16.2036	0.0396
2454122.35605	16.1915	0.04
2454122.35816	16.2275	0.0426
2454122.36026	16.2256	0.0419

Table 3—Continued

JD (1)	R-Mag. (2)	σ (3)
2454124.17064	15.7461	0.0441
2454124.17273	15.7925	0.0481
2454124.17484	15.7756	0.0417
2454124.17694	15.7634	0.0454
2454124.18115	15.7924	0.0415
2454124.18325	15.7806	0.0345
2454124.18535	15.8003	0.032
2454124.18956	15.7907	0.033
2454124.19166	15.7991	0.0318
2454124.19376	15.7789	0.0331
2454124.19587	15.7612	0.0298
2454124.19797	15.762	0.0298
2454124.20007	15.7104	0.0298
2454124.20218	15.746	0.0275
2454124.20428	15.739	0.0292
2454124.20638	15.7471	0.0295
2454124.20848	15.7325	0.0272
2454124.21059	15.7403	0.0278
2454124.21269	15.7521	0.0279
2454124.21479	15.7532	0.0279
2454124.21689	15.7082	0.0273
2454124.21899	15.6798	0.026
2454124.22110	15.6691	0.0266
2454124.23730	15.6789	0.0561
2454124.23941	15.6624	0.0463
2454124.24573	15.6201	0.0396
2454124.24993	15.6483	0.0355
2454124.25202	15.6605	0.0371
2454124.25413	15.693	0.034
2454124.25624	15.6773	0.031
2454124.25833	15.6917	0.0293
2454124.26044	15.6962	0.0345
2454124.26255	15.6632	0.0315
2454124.26464	15.6571	0.0283
2454124.26675	15.6455	0.028
2454124.26885	15.6538	0.0275
2454124.27095	15.6758	0.0276
2454124.27306	15.6938	0.03
2454124.27516	15.6967	0.0284
2454124.27726	15.6892	0.0304
2454124.27936	15.6844	0.0311
2454124.28148	15.6456	0.0311
2454124.28358	15.6297	0.0308
2454124.28568	15.6477	0.029
2454124.29541	15.6674	0.031

Table 3—Continued

JD (1)	R-Mag. (2)	σ (3)
2454124.29750	15.6911	0.0322
2454124.29961	15.691	0.0334
2454124.30171	15.6615	0.0417
2454124.30381	15.6359	0.0363
2454124.30591	15.6422	0.035
2454124.30802	15.6202	0.0336
2454124.31012	15.6442	0.0375
2454124.31222	15.616	0.0391
2454124.31433	15.6354	0.0463
2454124.31642	15.6252	0.0507
2454124.32064	15.6385	0.048
2454124.32273	15.6747	0.0563
2454124.32484	15.8024	0.0825
2454124.32694	15.6955	0.0651
2454124.32905	15.6011	0.0538
2454124.33116	15.5054	0.0646
2454124.33326	15.4899	0.0761
2454124.33746	15.6576	0.0966
2454124.34167	15.6389	0.0647
2454124.36270	15.7688	0.1142
2454125.25856	16.1169	0.0387
2454125.26067	16.1068	0.0431
2454125.26277	16.1037	0.0413
2454125.26487	16.0663	0.0376
2454125.26697	16.0596	0.0389
2454125.27024	15.9968	0.0361
2454125.27446	16.0944	0.0445
2454125.27656	16.0407	0.0356
2454125.27867	16.0469	0.042
2454125.28076	16.0128	0.0402
2454125.28287	16.0439	0.0369
2454125.28498	16.0599	0.0407
2454125.28707	16.0929	0.0388
2454125.28918	16.0965	0.0373
2454125.29128	16.0764	0.0409
2454125.29338	16.0815	0.0386
2454125.29549	16.0703	0.0387
2454125.30163	16.04	0.0358
2454125.30374	16.0385	0.0406
2454125.30584	15.9964	0.0349
2454125.30794	15.9406	0.0356
2454125.31005	15.9452	0.0374
2454125.31215	15.9976	0.0364
2454125.31425	16.0392	0.038
2454125.31635	16.0716	0.038

Table 3—Continued

JD (1)	R-Mag. (2)	σ (3)
2454125.31846	16.0311	0.0396
2454125.32056	15.9887	0.0363
2454125.32266	15.9676	0.0352
2454125.32478	15.9873	0.0384
2454125.32687	16.0306	0.0397
2454125.32898	16.0653	0.0396
2454125.33109	16.0796	0.0409
2454125.34242	16.0372	0.0442
2454125.34451	16.0242	0.0422
2454125.34662	16.0428	0.0434
2454125.34873	16.0361	0.0422
2454125.35082	16.0531	0.0899
2454133.29643	15.8347	0.055
2454133.29854	15.8396	0.0579
2454133.30064	15.9113	0.0647
2454133.30274	15.8615	0.0565
2454133.30485	15.8896	0.0521
2454133.30694	15.8171	0.0431
2454133.30905	15.8987	0.0488
2454133.31116	15.8914	0.0468
2454133.31325	15.8903	0.047
2454133.31536	15.809	0.0423
2454133.31745	15.8422	0.0426
2454133.31956	15.9124	0.0482
2454133.32167	15.8521	0.0447
2454133.32376	15.8132	0.0451
2454133.32587	15.8319	0.0479
2454133.32797	15.85	0.052
2454133.33007	15.848	0.0539
2454133.33218	15.9356	0.0628
2454133.33429	15.746	0.0617
2454133.33639	15.7069	0.0738
2454133.33849	15.7707	0.0696
2454140.24811	15.3989	0.0225
2454140.25022	15.3957	0.0218
2454140.25233	15.38	0.0238
2454140.25442	15.3734	0.0242
2454140.25653	15.3811	0.0237
2454140.25862	15.4034	0.0243
2454140.26037	15.4115	0.0251
2454140.26248	15.4493	0.0245
2454140.26458	15.4395	0.0303
2454140.26668	15.418	0.0311
2454140.26878	15.3767	0.0292
2454140.27088	15.3516	0.0321

Table 3—Continued

JD (1)	R-Mag. (2)	σ (3)
2454140.27299	15.3532	0.03
2454140.27509	15.38	0.0284
2454140.27719	15.3952	0.0274
2454140.27929	15.3505	0.0244
2454140.28140	15.3746	0.0239
2454140.28351	15.3758	0.0233
2454140.29806	15.3268	0.0262
2454140.32119	15.3906	0.0393
2454140.32329	15.3866	0.025
2454140.32539	15.3566	0.0277
2454140.32750	15.3328	0.025
2454141.18918	15.7535	0.0306
2454141.19129	15.7116	0.0276
2454141.19339	15.7146	0.0269
2454141.19549	15.7171	0.0274
2454141.19759	15.7222	0.027
2454141.19969	15.7215	0.026
2454141.20179	15.6925	0.0275
2454141.20390	15.7349	0.0298
2454141.20600	15.7529	0.0273
2454141.20810	15.7446	0.0288
2454141.21021	15.7528	0.0301
2454141.21230	15.7109	0.0272
2454141.21441	15.7114	0.0261
2454141.21650	15.7163	0.0275
2454141.21861	15.7155	0.0267
2454141.22071	15.7271	0.0295
2454141.22281	15.7508	0.0268
2454141.22492	15.759	0.0271
2454141.22701	15.7007	0.0271
2454141.23885	15.6744	0.0229
2454141.24096	15.6771	0.0262
2454141.24307	15.7078	0.0257
2454141.24516	15.755	0.0243
2454141.24727	15.718	0.0243
2454141.24938	15.7168	0.0243
2454141.25147	15.6807	0.0232
2454141.25358	15.6893	0.0243
2454141.25568	15.7117	0.0238
2454141.25778	15.7631	0.0264
2454141.25988	15.7697	0.0264
2454141.26199	15.7612	0.0264
2454141.26409	15.7635	0.0262
2454141.26619	15.7512	0.0269
2454141.26829	15.7509	0.0276

Table 3—Continued

JD (1)	R-Mag. (2)	σ (3)
2454141.27039	15.731	0.0277
2454141.27250	15.7356	0.028
2454141.27459	15.7559	0.0279
2454141.27670	15.7539	0.0277
2454141.27881	15.7223	0.0282
2454141.28091	15.7112	0.0242
2454141.28302	15.7128	0.0256
2454141.28512	15.7528	0.0274
2454141.28722	15.7427	0.0273
2454141.28932	15.6974	0.027
2454141.29890	15.7174	0.0321
2454141.30100	15.6742	0.0332
2454141.30310	15.6773	0.0326
2454141.30521	15.7034	0.0334
2454142.19569	15.7945	0.0151
2454142.19780	15.8084	0.0153
2454142.20201	15.7766	0.0153
2454142.20623	15.7876	0.0155
2454142.20833	15.807	0.0152
2454142.21043	15.7827	0.0152
2454142.21464	15.7731	0.0149
2454142.21674	15.7556	0.0148
2454142.21884	15.7955	0.015
2454142.22095	15.7705	0.0147
2454142.22304	15.7892	0.0146
2454142.22885	15.7708	0.0159
2454142.23096	15.7904	0.0145
2454142.23307	15.7631	0.0145
2454142.23516	15.7878	0.014
2454142.23727	15.7842	0.014
2454142.23939	15.7735	0.0139
2454142.24148	15.7849	0.0144
2454142.24359	15.7998	0.0143
2454142.24568	15.7943	0.0141
2454142.24779	15.8179	0.0143
2454142.24990	15.8142	0.0145
2454142.25199	15.801	0.0139
2454142.25410	15.8037	0.0139
2454142.25620	15.7976	0.0139
2454142.25830	15.8304	0.0139
2454142.26040	15.8227	0.0144
2454142.26250	15.8331	0.0146
2454142.26461	15.8167	0.0146
2454142.26671	15.8113	0.0146
2454142.26881	15.8346	0.0146

Table 3—Continued

JD (1)	R-Mag. (2)	σ (3)
2454142.27091	15.8199	0.0148
2454142.27302	15.827	0.0148
2454142.28005	15.7983	0.0157
2454142.28215	15.8148	0.0156
2454142.28426	15.8007	0.0152
2454142.28637	15.8277	0.0152
2454142.28846	15.8276	0.0154
2454142.29057	15.8366	0.0159
2454142.29267	15.8244	0.0163
2454142.29477	15.8111	0.0156
2454142.29688	15.8214	0.0155
2454142.29898	15.8244	0.0157
2454142.30108	15.8182	0.0163
2454142.30318	15.8204	0.0164
2454142.30529	15.8362	0.017
2454142.30738	15.8337	0.0168
2454142.31369	15.8001	0.0161
2454142.31580	15.8429	0.0158
2454142.31790	15.8474	0.0152
2454142.32000	15.8276	0.0151
2454142.32211	15.8608	0.0155
2454142.32421	15.8331	0.0143
2454143.17964	15.734	0.0278
2454143.18175	15.7509	0.0266
2454143.18385	15.801	0.0279
2454143.18595	15.7707	0.0281
2454143.18806	15.7576	0.0281
2454143.19016	15.7282	0.0253
2454143.19226	15.6988	0.0259
2454143.19436	15.7356	0.026
2454143.19647	15.7137	0.0238
2454143.19857	15.7447	0.026
2454143.20067	15.762	0.0269
2454143.20277	15.791	0.0293
2454143.20487	15.7997	0.0335
2454143.20698	15.8336	0.0449
2454143.20907	15.8266	0.0574
2454143.21118	15.8155	0.0802
2454143.29441	15.7113	0.0406
2454143.29652	15.6785	0.0348
2454143.29861	15.6684	0.0288
2454144.21106	15.8711	0.0145
2454144.21317	15.8434	0.0157
2454144.21528	15.8155	0.0157
2454144.21948	15.8755	0.0193

Table 3—Continued

JD (1)	R-Mag. (2)	σ (3)
2454144.22159	15.8289	0.0184
2454144.22369	15.8443	0.0221
2454144.22579	15.8221	0.0241
2454144.23000	15.8166	0.029
2454144.23211	15.8245	0.0306
2454144.23420	15.7837	0.0448
2454144.23631	15.8089	0.0352
2454144.23841	15.7673	0.0261
2454144.24052	15.8274	0.0313
2454144.24262	15.7956	0.0263
2454144.24472	15.7875	0.025
2454144.24683	15.7987	0.0235
2454144.24894	15.8164	0.0173
2454144.25314	15.8108	0.0145
2454144.25524	15.8063	0.0144
2454144.25734	15.798	0.0154
2454144.25944	15.7794	0.0187
2454144.26155	15.8031	0.0324
2454144.26365	15.7757	0.0437
2454144.26575	15.7793	0.0387
2454144.26786	15.8165	0.0417
2454144.26997	15.8037	0.0633
2454144.27662	15.8263	0.046
2454144.27873	15.8785	0.0625
2454144.28083	15.8268	0.0721
2454145.17705	15.7395	0.0269
2454145.18336	15.7237	0.0258
2454145.18545	15.7386	0.0282
2454145.18756	15.7612	0.0269
2454145.18966	15.7571	0.0255
2454145.19388	15.7755	0.023
2454145.19598	15.7789	0.0189
2454145.19809	15.7879	0.0169
2454145.20019	15.7699	0.0161
2454145.20229	15.7994	0.0171
2454145.20651	15.7875	0.0189
2454145.20860	15.7634	0.022
2454145.21071	15.7824	0.0251
2454145.21492	15.7658	0.026
2454145.21701	15.7594	0.0258
2454145.21912	15.774	0.0235
2454145.22333	15.7368	0.0204
2454145.22754	15.7395	0.0188
2454145.22964	15.7434	0.0195
2454145.23175	15.7566	0.0187

Table 3—Continued

JD (1)	R-Mag. (2)	σ (3)
2454145.23595	15.7926	0.0182
2454145.23806	15.7688	0.0187
2454145.24016	15.779	0.02
2454145.24226	15.7699	0.0223
2454145.24436	15.7659	0.0217
2454145.24647	15.7705	0.0219
2454145.24857	15.7223	0.0205
2454145.25067	15.7878	0.02
2454145.25278	15.7392	0.0201
2454145.25488	15.7401	0.0208
2454145.25698	15.7416	0.02
2454145.25909	15.7347	0.0194
2454145.26119	15.7302	0.0188
2454145.26330	15.7374	0.0197
2454145.26541	15.7262	0.0207
2454145.26751	15.7219	0.0208
2454145.27171	15.7358	0.0185
2454145.27844	15.7157	0.0189
2454145.28265	15.7523	0.0237
2454145.28474	15.7729	0.028
2454145.28685	15.7386	0.0276
2454145.28896	15.7449	0.0285
2454145.29108	15.7469	0.0272
2454145.29317	15.7588	0.0254
2454145.29528	15.7572	0.0214
2454145.29738	15.7266	0.0192
2454145.29949	15.736	0.0179
2454145.30159	15.7421	0.0176
2454145.30580	15.7981	0.0201
2454145.30789	15.7409	0.0215
2454145.31000	15.7604	0.0237
2454145.31211	15.709	0.0259
2454145.31631	15.7295	0.0255
2454145.31841	15.7423	0.0244
2454145.32052	15.7295	0.0246
2454145.32263	15.7352	0.0236
2454146.16865	15.8491	0.0089
2454146.17462	15.8611	0.0097
2454146.17810	15.8552	0.0096
2454146.18160	15.8515	0.0096
2454146.18509	15.8541	0.0094
2454146.18858	15.8587	0.0097
2454146.19207	15.8631	0.0095
2454146.19557	15.8664	0.0096
2454146.27306	15.7988	0.0229

Table 3—Continued

JD (1)	R-Mag. (2)	σ (3)
2454146.27516	15.8751	0.0249
2454146.27727	15.8663	0.0254
2454146.27937	15.8794	0.0272
2454146.28147	15.8687	0.0243
2454146.28358	15.8528	0.025
2454146.28568	15.84	0.0253
2454146.28779	15.8317	0.0258
2454146.28988	15.835	0.0254
2454146.29199	15.8592	0.0259
2454146.29410	15.888	0.028
2454146.29619	15.8279	0.0257
2454146.30040	15.8598	0.0268
2454146.30251	15.872	0.0278
2454146.30637	15.8884	0.0291
2454146.30846	15.9107	0.0321
2454146.31057	15.8449	0.0278
2454146.31267	15.8351	0.0308
2454146.31479	15.8243	0.0295
2454146.31689	15.8256	0.03
2454146.31899	15.8219	0.0336
2454148.28935	15.4602	0.0309
2454148.29145	15.5125	0.1262
2454148.29355	15.4608	0.0389
2454148.29565	15.4379	0.029
2454148.29776	15.4533	0.0315
2454148.29986	15.4587	0.0295
2454151.25354	14.4321	0.0107
2454151.25565	14.4152	0.0114
2454151.25774	14.4145	0.0111
2454151.25985	14.4407	0.0113
2454151.26196	14.4341	0.0118
2454151.26405	14.4237	0.0112
2454151.26616	14.4205	0.0114
2454151.26826	14.4234	0.0107
2454151.27036	14.4439	0.0116
2454151.27246	14.4491	0.0117
2454151.27457	14.4316	0.0114
2454151.27667	14.4304	0.0116
2454151.27877	14.4226	0.0123
2454151.28088	14.443	0.0119
2454151.28297	14.4344	0.012
2454151.28508	14.4311	0.0123
2454151.28719	14.4288	0.0119
2454151.28928	14.4168	0.0135
2454151.29139	14.4034	0.0119

Table 3—Continued

JD (1)	R-Mag. (2)	σ (3)
2454151.29349	14.3738	0.012
2454157.17744	14.9275	0.0101
2454157.18164	14.9186	0.0102
2454157.18375	14.9071	0.0097
2454157.18585	14.9162	0.0102
2454157.18795	14.9349	0.01
2454157.19006	14.9269	0.0097
2454157.19215	14.9351	0.0098
2454157.19426	14.9316	0.0099
2454157.19637	14.9173	0.01
2454157.19846	14.9422	0.0101
2454157.20057	14.936	0.0105
2454157.20266	14.9482	0.0105
2454157.20477	14.9441	0.0102
2454157.20689	14.9446	0.0107
2454157.20898	14.9329	0.0105
2454157.21109	14.9319	0.011
2454157.21529	14.9279	0.0108
2454157.21740	14.933	0.0103
2454157.21949	14.9344	0.0111
2454157.22160	14.9382	0.011
2454157.22369	14.9091	0.0111
2454157.22580	14.9225	0.0114
2454157.22791	14.9229	0.0118
2454157.23000	14.9183	0.0125
2454157.23211	14.9401	0.0113
2454157.23420	14.9335	0.0117
2454157.23631	14.9428	0.0117
2454157.23841	14.9421	0.0118
2454157.24051	14.9558	0.0121
2454157.24262	14.9299	0.0118
2454157.24471	14.9322	0.0123
2454157.24682	14.9339	0.0126
2454157.24892	14.9437	0.0128
2454157.25102	14.9619	0.0122
2454157.25312	14.9608	0.0125
2454157.25523	14.9323	0.012
2454157.25734	14.9307	0.0129
2454157.25944	14.9308	0.0129
2454157.26154	14.9372	0.0129
2454157.26569	14.9294	0.014
2454157.26779	14.9349	0.0145
2454157.26990	14.9296	0.0149
2454157.27200	14.9399	0.0141
2454157.27411	14.9433	0.0144

Table 3—Continued

JD (1)	R-Mag. (2)	σ (3)
2454157.27620	14.933	0.014
2454157.27831	14.9379	0.0136
2454157.28040	14.9273	0.0135
2454157.28251	14.9371	0.0145
2454157.28462	14.8942	0.0145
2454157.28671	14.9492	0.0153
2454157.28882	14.9427	0.0164
2454157.29093	14.946	0.0175
2454168.20370	15.2095	0.0182
2454168.20581	15.1935	0.0181
2454168.20791	15.2314	0.0197
2454168.21001	15.2177	0.0212
2454168.21632	15.2146	0.0249
2454168.21843	15.2222	0.0206
2454168.22053	15.2411	0.0208
2454169.19086	15.2719	0.0254
2454169.19716	15.2892	0.0283
2454169.19927	15.3071	0.0218
2454169.20138	15.2786	0.0214
2454169.20347	15.3055	0.0194
2454169.20558	15.3156	0.0206
2454169.21609	15.3143	0.0202
2454169.21819	15.3279	0.0199
2454169.22029	15.3336	0.0212
2454169.22240	15.3309	0.0211
2454169.22450	15.3169	0.0204
2454169.22660	15.3074	0.0208
2454169.22870	15.248	0.0214
2454170.23333	15.5003	0.0255
2454170.23544	15.4579	0.0257
2454170.23755	15.4638	0.0258
2454170.24176	15.5092	0.0285
2454170.24385	15.4909	0.0261
2454170.24596	15.4995	0.0261
2454170.24807	15.4818	0.0272
2454170.25016	15.4452	0.028
2454170.25227	15.4882	0.031
2454170.25438	15.4986	0.033
2454170.25647	15.4333	0.0297
2454171.20607	15.6349	0.0262
2454171.20817	15.6282	0.0259
2454171.21027	15.6324	0.0277
2454171.21237	15.6732	0.0276
2454171.21448	15.6661	0.0268
2454171.21657	15.6663	0.0297

Table 3—Continued

JD (1)	R-Mag. (2)	σ (3)
2454171.21868	15.6471	0.0289
2454171.22079	15.6686	0.0283
2454171.22288	15.7054	0.0288
2454171.22499	15.6918	0.0274
2454171.22710	15.6936	0.0298
2454171.22919	15.6658	0.0291
2454171.23130	15.6357	0.0286
2454171.23340	15.643	0.0302
2454171.23550	15.6336	0.028
2454171.23760	15.6568	0.0295
2454171.23971	15.6604	0.0316
2454171.24181	15.6737	0.0331
2454171.24391	15.6404	0.0311
2454171.24602	15.6379	0.033
2454171.24811	15.7091	0.0356
2454171.25022	15.6262	0.0344
2454171.25233	15.6013	0.0336
2454171.25442	15.6257	0.0343
2454174.22213	15.6441	0.0375
2454174.22424	15.6515	0.0424
2454174.22633	15.6033	0.0373
2454174.22844	15.5678	0.0416
2454174.23054	15.6311	0.047
2454174.23264	15.6098	0.0452
2454174.23475	15.6682	0.048
2454174.23685	15.6553	0.0483
2454174.23896	15.7364	0.0538
2454174.24105	15.6846	0.0482
2454179.22104	15.9183	0.028
2454179.22525	15.9271	0.0292
2454179.22736	15.9483	0.0276
2454179.22947	15.876	0.0262
2454179.23157	15.8763	0.0298
2454179.23578	15.9194	0.0349
2454180.23375	16.0837	0.0682
2454180.23585	15.9806	0.0677
2454190.20384	15.7223	0.057
2454190.20595	15.6887	0.0614
2454190.20806	15.5333	0.0551
2454190.21436	15.5738	0.0694
2454415.41053	17.7246	0.07
2454415.41402	17.7159	0.0703
2454421.42663	17.2025	0.0439
2454421.43013	17.183	0.0411
2454486.25142	16.8427	0.0649

Table 3—Continued

JD (1)	R-Mag. (2)	σ (3)
2454486.25353	16.8104	0.0638
2454486.25563	16.7592	0.0811
2454486.25773	16.8718	0.0754
2454486.25984	16.8897	0.0558
2454489.19351	16.9724	0.0341
2454489.19561	16.9317	0.0323
2454489.19772	16.9019	0.0356
2454489.19983	16.9471	0.0363
2454499.22863	16.8926	0.0224
2454499.23073	16.8749	0.022
2454499.23284	16.8822	0.0208
2454499.23494	16.8946	0.0223
2454502.20632	17.5851	0.037
2454502.20843	17.6878	0.0391
2454502.21052	17.6599	0.0403
2454502.21263	17.6704	0.0391
2454522.23718	17.778	0.0532
2454522.23928	17.7654	0.0512
2454522.24139	17.824	0.0565
2454522.24348	17.8177	0.0558
2454649.49354	16.9621	0.0476
2454649.49565	16.9066	0.0427
2454649.49775	16.945	0.054
2454649.49985	16.8925	0.0522
2454649.50826	16.9226	0.0565
2454649.51037	17.0138	0.0592
2454650.50302	16.7477	0.0387
2454650.50513	16.7907	0.04
2454650.50723	16.7809	0.0418
2454651.49640	16.7126	0.0393
2454651.49849	16.8013	0.0441
2454651.50060	16.7575	0.0678
2454651.50271	16.6796	0.0483
2454651.50480	16.7662	0.0528
2454651.50691	16.769	0.0435
2454652.48818	16.729	0.0353
2454652.49029	16.7503	0.035
2454652.49238	16.6988	0.0345
2454652.49660	16.7401	0.0329
2454652.49869	16.7295	0.0348
2454652.50080	16.7247	0.0298
2454652.50291	16.7305	0.0359
2454652.50500	16.6754	0.0353
2454652.50711	16.6668	0.0361
2454654.51241	16.0455	0.0234

Table 3—Continued

JD (1)	R-Mag. (2)	σ (3)
2454654.51661	16.0183	0.028
2454654.51871	16.0222	0.028
2454654.52082	16.0739	0.0316
2454654.52292	16.0853	0.0361
2454654.52502	16.1222	0.0504
2454656.49708	15.7101	0.0157
2454656.49918	15.717	0.0163
2454656.50128	15.7231	0.0146
2454656.50339	15.7381	0.0151
2454657.50993	15.8167	0.0373
2454687.53931	17.4371	0.0482
2454687.54141	17.4436	0.0495
2454687.54352	17.3781	0.0558
2454687.54561	17.4109	0.07
2454706.54415	16.2592	0.0205
2454706.54626	16.2433	0.0171
2454706.54837	16.2027	0.0169
2454706.55046	16.2198	0.0207
2454707.48043	16.2305	0.0225
2454707.48254	16.1961	0.0199
2454707.48463	16.206	0.0202
2454709.51538	16.3975	0.0315
2454709.51748	16.3647	0.0246
2454709.51958	16.3445	0.0283
2454709.52169	16.363	0.0411
2454711.50341	16.1123	0.0168
2454711.50552	16.1195	0.0151
2454711.50762	16.1267	0.0163
2454711.50972	16.1494	0.017
2454716.47584	15.6677	0.0122
2454716.47795	15.6503	0.0123
2454716.48006	15.6513	0.012
2454716.48215	15.6621	0.0134
2454716.48426	15.6586	0.0135
2454716.48637	15.6515	0.0171
2454722.52293	15.5264	0.0107
2454722.52924	15.5358	0.0116
2454723.52624	15.6305	0.015
2454723.53256	15.602	0.0141
2454725.37651	15.3685	0.0221
2454725.37791	15.3644	0.0213
2454725.37932	15.3693	0.0215
2454725.38073	15.3589	0.0211
2454725.38213	15.3706	0.0217
2454725.38354	15.3649	0.0213

Table 3—Continued

JD (1)	R-Mag. (2)	σ (3)
2454725.38495	15.3499	0.0214
2454725.38637	15.3876	0.0219
2454726.40641	14.8648	0.0192
2454726.40782	14.841	0.0187
2454726.40923	14.8617	0.0191
2454726.41064	14.8759	0.0191
2454726.41346	14.8467	0.0187
2454726.41486	14.8792	0.0181
2454726.41627	14.8683	0.0185
2454726.41769	14.8664	0.0185
2454726.41909	14.8658	0.0179
2454729.35012	15.2822	0.0516
2454729.35118	15.3065	0.0529
2454729.35225	15.2764	0.0513
2454729.35331	15.3626	0.0565
2454729.35436	15.2123	0.0496
2454729.35543	15.2428	0.0516
2454729.35651	15.2583	0.0504
2454729.35757	15.2808	0.0483
2454729.35863	15.3287	0.0533
2454729.35969	15.3126	0.0533
2454729.36075	15.2281	0.0521
2454729.36182	15.3034	0.0501
2454729.36287	15.2805	0.048
2454729.36393	15.285	0.0458
2454729.36500	15.3197	0.0465
2454729.36607	15.3372	0.0463
2454729.36712	15.2576	0.0469
2454729.36818	15.2742	0.0459
2454729.36925	15.2584	0.0488
2454729.37030	15.1928	0.0451
2454729.37137	15.2059	0.0462
2454729.37243	15.2515	0.0462
2454729.37348	15.2387	0.0473
2454729.37455	15.2577	0.0465
2454729.37561	15.2611	0.0465
2454729.37667	15.2278	0.0691
2454729.37773	15.2987	0.0871
2454729.56326	15.426	0.0428
2454729.56432	15.4061	0.0445
2454729.56538	15.383	0.0416
2454729.56645	15.5048	0.044
2454729.56751	15.3949	0.0398
2454729.57019	15.4131	0.0522
2454729.57125	15.4721	0.0473

Table 3—Continued

JD (1)	R-Mag. (2)	σ (3)
2454729.57232	15.4978	0.0464
2454729.57337	15.4014	0.0482
2454729.57443	15.4323	0.048
2454729.57550	15.468	0.0569
2454729.57655	15.5121	0.056
2454729.57762	15.365	0.0555
2454729.57868	15.3267	0.0597
2454729.57973	15.4354	0.0588
2454729.58080	15.3366	0.0896
2454729.58186	15.4614	0.1147
2454729.58293	15.3942	0.0661
2454729.58398	15.4465	0.0652
2454730.35132	15.2664	0.0237
2454730.35238	15.217	0.0246
2454730.35395	15.2451	0.0189
2454730.35535	15.2485	0.0189
2454730.35676	15.2251	0.0194
2454730.35817	15.213	0.0188
2454730.35957	15.2413	0.0189
2454730.36098	15.2233	0.0188
2454730.36240	15.2171	0.0185
2454730.36380	15.2045	0.0187
2454730.36521	15.2105	0.0182
2454730.36662	15.2204	0.0184
2454730.36802	15.2069	0.0186
2454730.36943	15.2545	0.0191
2454730.37102	15.2311	0.0195
2454730.37242	15.223	0.0184
2454730.37383	15.245	0.0192
2454730.37640	15.2518	0.0187
2454730.37884	15.2404	0.0168
2454730.38026	15.2454	0.0167
2454730.38167	15.2357	0.018
2454730.38319	15.2291	0.0185
2454730.38461	15.2325	0.0174
2454730.38601	15.2264	0.0169
2454730.38742	15.2372	0.0184
2454730.38883	15.2388	0.0181
2454730.39023	15.2056	0.0184
2454730.39164	15.2089	0.0183
2454730.39306	15.2239	0.0182
2454730.39447	15.2188	0.0169
2454730.39587	15.2214	0.0167
2454730.39728	15.2031	0.0172
2454730.39869	15.1878	0.0169

Table 3—Continued

JD (1)	R-Mag. (2)	σ (3)
2454730.41734	15.1983	0.0174
2454730.43412	15.1893	0.0365
2454730.43553	15.1778	0.0354
2454730.43694	15.1584	0.0207
2454730.43836	15.1954	0.0194
2454730.43976	15.1663	0.0171
2454730.44117	15.1666	0.0172
2454730.44258	15.1743	0.0174
2454730.44399	15.1656	0.0156
2454730.44539	15.144	0.0163
2454730.44681	15.1552	0.0171
2454730.44822	15.1426	0.0174
2454730.44962	15.1599	0.0188
2454731.57780	14.7474	0.0258
2454731.57920	14.685	0.0467
2454731.58061	14.6959	0.0125
2454731.58202	14.7004	0.0205
2454731.58343	14.7109	0.0129
2454731.58484	14.7218	0.0136
2454731.58625	14.7066	0.0136
2454731.58765	14.7211	0.0156
2454731.58906	14.691	0.0149
2454731.59048	14.6753	0.0166
2454733.48182	14.245	0.007
2454733.48323	14.241	0.007
2454733.48463	14.239	0.007
2454733.48604	14.242	0.007
2454733.48745	14.241	0.007
2454733.48885	14.236	0.007
2454733.49027	14.246	0.007
2454733.49168	14.249	0.007
2454733.56799	14.202	0.01
2454733.57080	14.192	0.015
2454733.57221	14.19	0
2454738.52675	15.6591	0.0129
2454738.52885	15.6579	0.0141
2454738.53095	15.6565	0.0136
2454738.53306	15.6536	0.0151
2454738.53516	15.6639	0.0144
2454738.53726	15.6653	0.0134
2454738.54147	15.6762	0.0141
2454739.48307	15.3633	0.0134
2454739.48516	15.3651	0.0125
2454739.48727	15.3462	0.0287
2454739.48937	15.2854	0.0454

Table 3—Continued

JD (1)	R-Mag. (2)	σ (3)
2454739.49358	15.3382	0.0553
2454739.49988	15.3693	0.0472
2454739.50199	15.3664	0.0228
2454741.44288	15.3991	0.0114
2454741.44499	15.3843	0.0105
2454742.53491	15.8923	0.0147
2454742.53700	15.8956	0.0139
2454742.53911	15.8782	0.0132
2454743.39089	16.0396	0.0148
2454743.39509	16.038	0.0171
2454743.39720	16.0507	0.0149
2454744.48819	15.6463	0.0122
2454744.49030	15.6394	0.0121
2454745.41038	15.8083	0.0124
2454745.41460	15.8054	0.0147
2454746.29418	15.8761	0.0162
2454746.29629	15.8823	0.0176
2454746.29838	15.8624	0.0164
2454746.30049	15.8661	0.0149
2454746.30259	15.8595	0.0146
2454747.52784	15.5713	0.018
2454747.53204	15.5746	0.0241
2454747.53414	15.5632	0.0232
2454750.52107	15.1764	0.0098
2454750.52316	15.1709	0.0089
2454750.52527	15.168	0.0091
2454752.35090	14.5575	0.015
2454752.35162	14.5751	0.0152
2454752.35234	14.5862	0.0147
2454752.35304	14.5847	0.0151
2454752.35376	14.5801	0.0147
2454752.35448	14.5771	0.015
2454752.35523	14.5562	0.0146
2454752.35594	14.5809	0.0148
2454752.35665	14.5531	0.0148
2454752.35737	14.5407	0.0148
2454752.35808	14.5558	0.0146
2454752.35880	14.5458	0.0147
2454752.35951	14.5568	0.0151
2454752.36022	14.5674	0.0146
2454752.36094	14.5586	0.0144
2454752.36166	14.5506	0.0147
2454752.36237	14.5758	0.0147
2454752.36308	14.5786	0.0143
2454752.36380	14.5686	0.0143

Table 3—Continued

JD (1)	R-Mag. (2)	σ (3)
2454752.36451	14.5508	0.0148
2454752.36522	14.5771	0.0146
2454752.36594	14.5653	0.0146
2454752.41334	14.5639	0.0137
2454752.41406	14.5487	0.0141
2454752.41478	14.5208	0.0139
2454752.41549	14.5422	0.0142
2454752.41620	14.5588	0.0144
2454752.41692	14.5303	0.0144
2454752.48965	14.5279	0.0143
2454752.49036	14.5134	0.0142
2454752.49108	14.4999	0.0143
2454752.49179	14.5317	0.015
2454752.49250	14.5244	0.0145
2454752.49322	14.5047	0.014
2454752.59601	14.4374	0.0099
2454752.59889	14.4384	0.0105
2454752.60030	14.4429	0.0114
2454753.32181	14.7286	0.0234
2454753.32493	14.6978	0.0394
2454753.32564	14.7072	0.0392
2454753.32635	14.7295	0.0396
2454753.32707	14.6515	0.0369
2454753.32778	14.7111	0.0396
2454753.32850	14.7173	0.0375
2454753.32921	14.7376	0.0722
2454753.32993	14.6908	0.0395
2454753.33064	14.6796	0.0457
2454753.33135	14.7205	0.0465
2454753.33207	14.7141	0.0367
2454753.33278	14.7222	0.0353
2454753.51481	14.684	0.0203
2454753.51623	14.678	0.0294
2454753.51763	14.6822	0.0187
2454753.51904	14.6872	0.019
2454753.52045	14.6859	0.0189
2454753.52186	14.6877	0.0191
2454753.52326	14.6873	0.0192
2454753.52468	14.7074	0.0192
2454754.30899	14.5247	0.0336
2454754.30971	14.5496	0.0342
2454754.31043	14.4864	0.0356
2454754.31113	14.5837	0.0349
2454754.31185	14.5487	0.034
2454754.31257	14.5253	0.0346

Table 3—Continued

JD (1)	R-Mag. (2)	σ (3)
2454754.31328	14.5139	0.0344
2454754.31399	14.4892	0.0341
2454754.31471	14.5017	0.0337
2454754.31543	14.5034	0.034
2454754.31613	14.4998	0.0328
2454754.31685	14.5046	0.0324
2454754.50785	14.3238	0.0344
2454754.50856	14.2979	0.033
2454754.50927	14.3185	0.0332
2454754.50999	14.31	0.0335
2454754.51071	14.3579	0.0345
2454754.51141	14.384	0.034
2454754.51213	14.332	0.034
2454754.51285	14.3258	0.035
2454757.29397	14.9715	0.0171
2454757.29538	14.9812	0.017
2454757.29679	14.982	0.0165
2454757.29884	14.9728	0.0157
2454757.30095	14.9863	0.0174
2454757.56361	15.0418	0.0168
2454757.56502	15.0329	0.0169
2454757.56643	15.0382	0.0161
2454757.56784	15.0271	0.016
2454757.56925	15.0444	0.0161
2454757.57066	15.0448	0.0162
2454759.34885	15.1282	0.0118
2454759.35096	15.1346	0.0119
2454759.35306	15.1184	0.0117
2454759.35516	15.1271	0.011
2454760.41170	15.263	0.01
2454760.41381	15.2589	0.0104
2454760.41590	15.2754	0.0102
2454760.41801	15.2791	0.0106
2454763.27639	15.4299	0.015
2454763.28059	15.4358	0.0213
2454763.28480	15.4325	0.0181
2454763.28698	15.3968	0.018
2454763.28909	15.4101	0.0157
2454763.29119	15.4362	0.0296
2454766.40238	15.3291	0.0101
2454766.40448	15.3045	0.0145
2454766.40659	15.3455	0.0106
2454766.41079	15.3342	0.0101
2454766.41289	15.3164	0.0141
2454766.41500	15.3344	0.01

Table 3—Continued

JD (1)	R-Mag. (2)	σ (3)
2454768.42552	15.3454	0.0098
2454768.42763	15.3522	0.0108
2454768.42973	15.3542	0.0097
2454768.43183	15.3451	0.0098
2454770.50718	15.4488	0.0126
2454770.50928	15.449	0.012
2454770.51139	15.4483	0.0122
2454770.51348	15.4355	0.0114
2454771.41032	15.3002	0.0093
2454771.41243	15.2791	0.0089
2454771.41454	15.289	0.0095
2454771.41664	15.2947	0.0085
2454772.49423	15.0375	0.009
2454772.49633	15.0232	0.0092
2454772.49844	15.0312	0.0098
2454772.50053	15.0057	0.0091
2454773.41515	15.2423	0.0091
2454773.41726	15.2352	0.0097
2454773.41935	15.2496	0.0097
2454773.42146	15.2473	0.0093
2454779.49686	16.1381	0.0237
2454779.49897	16.1641	0.0239
2454779.50107	16.1334	0.0233
2454779.50317	16.1387	0.0211
2454779.50528	16.121	0.02
2454779.50737	16.1464	0.0268
2454780.45352	16.2782	0.0457
2454780.45493	16.2542	0.0402
2454780.45774	16.2742	0.0448
2454781.27346	16.2988	0.0562
2454781.27769	16.2754	0.0561
2454781.27910	16.3117	0.0574
2454781.28191	16.3174	0.0531
2454781.28332	16.2822	0.0521
2454785.40198	16.521	0.071
2454785.40339	16.3637	0.0639
2454785.40480	16.452	0.065
2454785.40622	16.3916	0.0633
2454785.40762	16.4647	0.0679
2454785.40903	16.5394	0.0735
2454785.41044	16.4525	0.0676
2454785.41184	16.523	0.0732
2454797.42920	16.1707	0.018
2454797.43131	16.1899	0.0181
2454797.43341	16.1935	0.0163

Table 3—Continued

JD (1)	R-Mag. (2)	σ (3)
2454797.43551	16.181	0.0151
2454797.43762	16.1825	0.0158
2454797.43972	16.2097	0.0166
2454799.43537	16.6364	0.0361
2454799.43748	16.6818	0.0587
2454800.41439	16.8513	0.0274
2454800.41649	16.8457	0.0259
2454800.41860	16.8116	0.0243
2454800.42071	16.8523	0.0259
2454802.19122	16.8421	0.0309
2454802.19332	16.8699	0.0306
2454802.19543	16.8706	0.0306
2454802.19752	16.8656	0.03
2454803.45476	16.7652	0.0254
2454803.45686	16.7245	0.026
2454803.45896	16.7474	0.0244
2454803.46106	16.7588	0.0255
2454804.45992	16.8457	0.0296
2454804.46201	16.7971	0.032
2454804.46412	16.7902	0.0311
2454804.46623	16.7959	0.0305
2454805.44682	16.9012	0.0306
2454805.44892	16.9062	0.0301
2454805.45103	16.9309	0.0296
2454805.45313	16.9148	0.0274
2454807.44036	16.8416	0.0306
2454807.44245	16.824	0.0334
2454807.44456	16.8382	0.0345
2454807.44667	16.8013	0.0299
2454807.44877	16.8163	0.0317
2454819.38042	17.0236	0.0438
2454819.38252	17.1027	0.0479
2454819.38463	16.9927	0.0438
2454819.38674	16.9955	0.0433
2454827.25183	16.5658	0.0198
2454827.25393	16.5828	0.021
2454827.25604	16.5568	0.0198
2454827.25815	16.5616	0.0194
2454834.35743	16.5922	0.0237
2454834.35954	16.5859	0.0235
2454834.36164	16.6238	0.0249
2454834.36375	16.6041	0.0248
2454834.36584	16.5807	0.0238
2454908.19721	17.2426	0.0594
2454908.19932	17.2228	0.0559

Table 3—Continued

JD (1)	R-Mag. (2)	σ (3)
2454908.20142	17.2625	0.0578
2454908.20352	17.3065	0.0625
2455006.49565	17.9007	0.1904
2455006.49774	18.3619	0.2741
2455006.50196	17.9747	0.2008
2455006.50487	18.148	0.4614
2455006.50910	17.7722	0.3236
2455048.51752	18.5359	0.2099
2455048.51962	18.3128	0.1511
2455068.55388	18.0956	0.1125
2455068.55598	18.1333	0.0984
2455071.52099	18.4222	0.1219
2455071.52310	18.2903	0.1047
2455093.54124	16.7576	0.0309
2455093.54335	16.7378	0.0273
2455093.54544	16.7694	0.0276
2455093.54755	16.7964	0.0289
2455093.54965	16.7846	0.0275
2455093.55176	16.7721	0.0278
2455093.55385	16.7844	0.029
2455093.55596	16.7898	0.029
2455093.55807	16.8103	0.0277
2455093.56017	16.814	0.0293
2455093.56227	16.8044	0.0324
2455093.56438	16.892	0.0456
2455093.56648	16.838	0.0574
2455093.56859	16.9496	0.0846
2455093.57068	17.0719	0.0908
2455095.56065	17.0768	0.0408
2455095.56275	17.021	0.0398
2455102.45998	17.4204	0.0615
2455120.34024	17.7002	0.0704
2455120.34235	17.646	0.067
2455144.22728	18.3104	0.1373
2455144.22939	18.1546	0.1019
2455160.31826	17.9646	0.117
2455160.32037	17.8251	0.0923
2455160.32248	17.8565	0.0982
2455160.32457	17.9777	0.1065
2455160.32668	18.0273	0.1111
2455160.32878	17.9762	0.0989
2455191.25807	17.9188	0.1072
2455391.52310	18.0451	0.1442
2455391.52589	17.9128	0.1437
2455413.50448	18.3756	0.1751

Table 3—Continued

JD (1)	R-Mag. (2)	σ (3)
2455413.50659	18.1461	0.1367
2455413.50868	18.3262	0.1679
2455413.51079	18.2694	0.1544
2455413.51289	18.2301	0.1532
2455415.51741	18.4245	0.1432
2455415.51951	18.3126	0.1268
2455416.50298	18.5111	0.1795
2455416.50508	18.1978	0.1398
2455416.50719	18.2324	0.1395
2455416.50929	18.4933	0.1688
2455419.48288	18.4249	0.1116
2455419.48499	18.426	0.1107
2455419.48919	18.5016	0.1186
2455427.49955	18.6711	0.1427
2455443.43244	18.479	0.1305
2455449.44141	18.5236	0.1001
2455449.44424	18.6814	0.1148
2455449.44634	18.7503	0.1263
2455479.41516	19.0695	0.5945
2455482.43199	18.2966	0.2642
2455482.43410	18.1986	0.2379
2455488.48545	18.0465	0.2064
2455488.48755	17.947	0.2012
2455488.48965	17.9334	0.1967
2455488.49387	17.8683	0.1806
2455488.49597	17.7453	0.156
2455497.47543	17.9912	0.2077
2455504.36493	18.3948	0.2807
2455508.32147	18.6756	0.4101
2455532.34271	18.5597	0.3558
2455532.34482	18.8235	0.4893
2455840.44080	18.2053	0.263
2455840.44290	18.2875	0.2888
2455841.43700	17.8881	0.1954
2455899.43145	17.2552	0.134
2455899.43355	17.2549	0.138
2455899.43566	17.2995	0.1456
2455899.43777	17.3205	0.15
2455900.36663	17.752	0.1041
2455900.36804	17.6778	0.0935
2455900.37086	17.729	0.0989
2455900.37227	17.6596	0.0989
2455907.26179	17.594	0.1918
2455907.26321	17.33	0.0946
2455907.26462	17.2259	0.077

Table 3—Continued

JD (1)	R-Mag. (2)	σ (3)
2455907.26603	17.328	0.0845
2455907.27103	17.513	0.1501
2455909.20306	17.889	0.0768
2455909.20649	17.8484	0.068
2455909.20859	17.8562	0.0764
2455909.21069	17.9585	0.0853
2455909.21280	17.931	0.0845
2455911.23302	17.8908	0.0721
2455911.23513	17.9548	0.077
2455911.23723	17.9039	0.0733
2455911.23934	17.9449	0.0708
2455911.24145	17.9067	0.07
2455970.20853	18.4693	0.1466
2455970.21064	18.5594	0.1578
2455970.21274	18.7113	0.1845
2455970.21485	18.741	0.1862
2455970.21696	18.5176	0.1472
2455970.21906	18.5093	0.1474
2455970.22117	18.3755	0.1291
2456164.54142	18.1133	0.1994
2456164.54353	18.0522	0.1964
2456166.47704	18.585	0.3224
2456166.47914	18.4217	0.2873
2456207.38302	17.6913	0.1386
2456207.38513	17.7373	0.1499
2456207.38723	17.7564	0.152
2456207.38934	17.7349	0.1476
2456217.44253	18.041	0.1663
2456217.44464	17.9177	0.1686
2456217.44675	18.0756	0.198
2456217.44885	18.1288	0.1815
2456236.36494	18.1589	0.2145
2456236.36705	18.0684	0.2063
2456247.35998	18.1014	0.2305
2456247.36210	18.23	0.2266
2456247.36420	18.4054	0.2631
2456247.36631	18.456	0.2759

Table 4. Radio Observations for AO 0235 + 164

JD (1)	$F_{4.8GHz}$ -Jy (2)	σ (3)
2454085.6533	0.8753	0.0078
2454085.6885	0.8744	0.0074
2454085.7237	0.8755	0.0075
2454085.7571	0.8746	0.0075
2454085.7901	0.8750	0.0075
2454085.8269	0.8897	0.0077
2454085.8608	0.8744	0.0078
2454086.5987	0.8764	0.0074
2454086.6333	0.8783	0.0075
2454086.6681	0.8767	0.0075
2454086.7032	0.8721	0.0074
2454086.7368	0.8839	0.0076
2454086.7701	0.8738	0.0075
2454086.8030	0.8706	0.0075
2454086.8368	0.8722	0.0077
2454087.4152	0.8651	0.0086
2454087.4414	0.8719	0.0086
2454087.4707	0.8680	0.0086
2454087.5002	0.8723	0.0085
2454087.5299	0.8688	0.0085
2454087.5569	0.8771	0.0086
2454087.5872	0.8746	0.0085
2454087.6178	0.8807	0.0087
2454087.6526	0.8790	0.0086
2454087.6876	0.8872	0.0087
2454087.7228	0.8796	0.0086
2454087.7562	0.8760	0.0086
2454087.7892	0.8719	0.0086
2454087.8260	0.8746	0.0087
2454088.4065	0.8767	0.0087
2454088.4327	0.8779	0.0087
2454088.4620	0.8697	0.0085
2454088.4913	0.8742	0.0086
2454088.5210	0.8803	0.0086
2454088.5561	0.8863	0.0087
2454088.5864	0.8758	0.0086
2454088.6171	0.8763	0.0086
2454088.6518	0.8894	0.0088
2454088.6869	0.8708	0.0088
2454088.7206	0.8711	0.0087
2454088.7539	0.8757	0.0087
2454088.8237	0.8680	0.0086
2454089.4038	0.8727	0.0088
2454089.4300	0.8717	0.0086
2454089.4593	0.8745	0.0086

Table 4—Continued

JD (1)	$F_{4.8GHz}$ -Jy (2)	σ (3)
2454089.4886	0.8752	0.0086
2454089.5183	0.8728	0.0086
2454089.5483	0.8815	0.0086
2454089.5754	0.8919	0.0088
2454089.6138	0.8868	0.0087
2454089.6486	0.8867	0.0087
2454089.6836	0.8770	0.0087
2454089.7173	0.8728	0.0086
2454089.7507	0.8736	0.0087
2454125.7260	0.8968	0.0079
2454126.3175	0.9125	0.0082
2454126.3469	0.8928	0.0079
2454126.3813	0.9083	0.0079
2454126.4157	0.9226	0.0079
2454126.4470	0.9045	0.0078
2454126.4795	0.8824	0.0077
2454126.5636	0.9260	0.0079
2454126.6047	0.9208	0.0079
2454126.6478	0.9246	0.0079
2454126.6911	0.9072	0.0079
2454126.7350	0.9322	0.0082
2454127.2988	0.9130	0.0084
2454127.3286	0.9025	0.0080
2454127.3631	0.9048	0.0079
2454127.3975	0.9108	0.0079
2454127.4320	0.9178	0.0079
2454127.4634	0.9136	0.0078
2454127.5027	0.9213	0.0080
2454127.5449	0.9233	0.0079
2454127.5904	0.9361	0.0081
2454127.6335	0.9248	0.0080
2454127.6767	0.9216	0.0080
2454127.7220	0.9264	0.0083
2454143.3745	0.9802	0.0092
2454143.4126	0.9918	0.0093
2454143.4536	0.9720	0.0092
2454143.4994	0.9621	0.0091
2454143.5418	0.9626	0.0091
2454143.5852	0.9319	0.0088
2454143.6322	0.9326	0.0089
2454143.6795	0.9127	0.0088
2454144.2518	0.9499	0.0092
2454144.2811	0.9507	0.0091
2454144.3186	0.9680	0.0095
2454144.3558	0.9703	0.0092

Table 4—Continued

JD (1)	$F_{4.8GHz}$ -Jy (2)	σ (3)
2454144.3969	0.9601	0.0090
2454144.4380	0.9677	0.0091
2454144.4837	0.9619	0.0091
2454144.5261	0.9605	0.0091
2454144.5701	0.9595	0.0091
2454144.6167	0.9675	0.0091
2454144.6640	0.9610	0.0092
2454145.2591	0.9414	0.0090
2454145.2884	0.9409	0.0090
2454145.3257	0.9489	0.0090
2454145.3630	0.9444	0.0089
2454145.4006	0.9498	0.0090
2454145.4418	0.9477	0.0089
2454145.4877	0.9437	0.0089
2454145.5301	0.9386	0.0089
2454145.5734	0.9578	0.0091
2454145.6204	0.9511	0.0090
2454145.6677	0.9523	0.0091
2454146.2394	0.9489	0.0092
2454146.2722	0.9489	0.0091
2454146.3095	0.9384	0.0089
2454146.3469	0.9414	0.0090
2454146.3879	0.9364	0.0088
2454146.4290	0.9420	0.0089
2454146.4747	0.9446	0.0089
2454146.5170	0.9334	0.0088
2454146.5584	0.9465	0.0089
2454146.6055	0.9298	0.0088
2454146.6490	0.9252	0.0088
2454146.6962	0.9187	0.0090
2454147.2838	0.9489	0.0090
2454147.3211	0.9596	0.0091
2454147.3584	0.9649	0.0091
2454183.2268	1.3745	0.0126
2454183.2641	1.3856	0.0127
2454183.2986	1.3870	0.0128
2454183.3365	1.4254	0.0130
2454183.3785	1.3485	0.0124
2454183.4266	1.3841	0.0128
2454183.4759	1.3815	0.0127
2454183.5253	1.3843	0.0128
2454183.5721	1.3393	0.0130
2454184.1485	1.3680	0.0127
2454184.1777	1.3814	0.0127
2454184.2150	1.3835	0.0127

Table 4—Continued

JD (1)	$F_{4.8GHz}$ -Jy (2)	σ (3)
2454184.2523	1.3755	0.0126
2454184.2899	1.3732	0.0126
2454184.3276	1.3506	0.0124
2454184.3696	1.3458	0.0124
2454184.4119	1.3774	0.0126
2454184.4590	1.3368	0.0123
2454184.5071	1.3214	0.0121
2454184.5609	1.2898	0.0120
2454185.1321	1.4101	0.0131
2454185.1612	1.4124	0.0130
2454185.1986	1.4079	0.0129
2454185.2359	1.3959	0.0128
2454185.2733	1.3955	0.0128
2454185.3079	1.4020	0.0147
2454185.3459	1.3857	0.0162
2454185.3881	1.4170	0.0140
2454185.4363	1.4196	0.0149
2454185.4855	1.5440	0.0316
2454185.5827	1.4447	0.0137
2454210.2704	2.1080	0.0226
2454210.3125	1.9940	0.0216
2454210.3606	1.9716	0.0214
2454210.4099	2.0133	0.0216
2454210.4594	1.9541	0.0212
2454211.0850	1.7794	0.0194
2454211.1173	1.7678	0.0192
2454211.1545	1.8591	0.0201
2454211.1919	1.9050	0.0205
2454211.2264	1.8281	0.0201
2454212.0619	2.0573	0.0224
2454212.0911	1.8663	0.0212
2454212.1659	1.9449	0.0218
2454212.2538	2.2041	0.0236
2454212.2958	2.0652	0.0221
2454212.3439	1.9248	0.0207
2454212.3931	2.0509	0.0220
2454212.4425	2.1332	0.0228
2454212.4897	2.0614	0.0221
2454213.0641	2.0079	0.0219
2454213.0933	2.0538	0.0223
2454213.1306	2.4026	0.0256
2454213.1679	2.2156	0.0239
2454213.2054	2.1191	0.0228
2454213.2401	2.1892	0.0235
2454213.2782	2.2282	0.0239

Table 4—Continued

JD (1)	$F_{4.8GHz}$ -Jy (2)	σ (3)
2454213.3204	2.3106	0.0247
2454213.3675	2.2071	0.0237
2454213.4169	2.2631	0.0244
2454213.4665	2.2314	0.0241
2454266.9211	2.5290	0.0241
2454266.9503	2.4675	0.0235
2454266.9876	2.4955	0.0237
2454267.0249	2.4865	0.0236
2454267.0624	2.5148	0.0239
2454267.1416	2.4928	0.0238
2454267.1794	2.5130	0.0239
2454267.2266	2.4975	0.0238
2454267.2768	2.5380	0.0243
2454267.3265	2.5632	0.0245
2454267.9322	2.3356	0.0223
2454267.9715	2.3733	0.0226
2454268.0091	2.3511	0.0223
2454268.0464	2.2836	0.0218
2454268.0809	2.3396	0.0222
2454268.1188	2.4004	0.0228
2454268.1609	2.3646	0.0225
2454268.2091	2.3657	0.0225
2454268.2584	2.4285	0.0231
2454268.2992	2.4356	0.0232
2454268.3463	2.4084	0.0230
2454268.9151	2.3839	0.0228
2454268.9443	2.3686	0.0226
2454268.9816	2.3552	0.0224
2454269.0240	2.3899	0.0227
2454269.0584	2.3824	0.0227
2454300.8157	2.3727	0.0225
2454300.8631	2.3557	0.0223
2454300.9113	2.3778	0.0225
2454300.9598	2.3850	0.0225
2454301.0052	2.3628	0.0223
2454301.0541	2.3838	0.0225
2454301.1033	2.3799	0.0225
2454301.1432	2.3828	0.0225
2454301.1795	2.4081	0.0228
2454301.1967	2.3962	0.0227
2454301.2365	2.3983	0.0227
2454301.2618	2.3741	0.0226
2454301.8090	2.3477	0.0223
2454301.8566	2.3704	0.0225
2454301.9048	2.3614	0.0223

Table 4—Continued

JD (1)	$F_{4.8GHz}$ -Jy (2)	σ (3)
2454301.9533	2.3637	0.0223
2454301.9986	2.4014	0.0227
2454302.0476	2.3486	0.0221
2454302.0968	2.3688	0.0224
2454302.1444	2.3659	0.0224
2454302.1806	2.3721	0.0224
2454302.2205	2.3897	0.0227
2454302.2601	2.3791	0.0228
2454302.8168	2.3171	0.0224
2454302.8643	2.3122	0.0221
2454302.9126	2.3089	0.0219
2454302.9612	2.2875	0.0217
2454303.0066	2.2814	0.0215
2454303.0556	2.2958	0.0217
2454303.1048	2.2772	0.0215
2454303.1446	2.3021	0.0218
2454303.1938	2.2997	0.0217
2454303.2414	2.2973	0.0219
2454303.2778	2.2977	0.0223
2454386.5880	1.4540	0.0125
2454386.6217	1.4501	0.0124
2454386.6647	1.4475	0.0123
2454386.7072	1.4383	0.0122
2454386.7465	1.4415	0.0123
2454386.7889	1.4476	0.0124
2454386.8351	1.4428	0.0123
2454386.8844	1.4375	0.0123
2454386.9272	1.4310	0.0125
2454386.9739	1.4262	0.0121
2454387.0213	1.4284	0.0123
2454387.5756	1.4075	0.0121
2454387.6092	1.4126	0.0121
2454387.6513	1.4087	0.0120
2454387.6937	1.4007	0.0119
2454387.7330	1.4085	0.0119
2454387.7754	1.4134	0.0120
2454387.8214	1.4083	0.0120
2454387.8713	1.4102	0.0120
2454387.9141	1.4133	0.0120
2454387.9608	1.4032	0.0119
2454388.0140	1.4136	0.0121
2454388.5713	1.4274	0.0123
2454388.6048	1.4389	0.0123
2454388.6487	1.4426	0.0123
2454388.6911	1.4521	0.0123

Table 4—Continued

JD (1)	$F_{4.8GHz}$ -Jy (2)	σ (3)
2454388.7303	1.4409	0.0122
2454388.7728	1.4454	0.0122
2454388.8188	1.4442	0.0122
2454388.8682	1.4413	0.0122
2454388.9110	1.4402	0.0122
2454388.9577	1.4366	0.0122
2454389.0083	1.4432	0.0123
2454456.3879	1.2136	0.0109
2454456.4142	1.2165	0.0108
2454456.4435	1.2184	0.0107
2454456.4778	1.2213	0.0107
2454456.5121	1.2304	0.0108
2454456.5433	1.2276	0.0108
2454456.5778	1.2477	0.0112
2454456.6168	1.2352	0.0109
2454456.6562	1.2536	0.0111
2454456.6987	1.2388	0.0111
2454456.7387	1.2445	0.0109
2454456.7823	1.2513	0.0110
2454456.8263	1.2599	0.0112
2454457.3962	1.3072	0.0116
2454457.4225	1.2954	0.0114
2454457.4569	1.3042	0.0114
2454457.4912	1.2951	0.0113
2454457.5256	1.3279	0.0117
2454457.5569	1.2876	0.0114
2454457.5916	1.2928	0.0116
2454457.6309	1.2898	0.0120
2454457.6733	1.2976	0.0118
2454457.7114	1.2914	0.0115
2454457.7549	1.2845	0.0112
2454457.7991	1.2683	0.0112
2454457.8427	1.2730	0.0114
2454458.3998	1.2589	0.0111
2454458.4281	1.2543	0.0110
2454458.4624	1.2396	0.0108
2454458.4967	1.2402	0.0110
2454458.5311	1.2528	0.0111
2454458.5660	1.2485	0.0111
2454458.6008	1.2726	0.0114
2454458.6406	1.2526	0.0117
2454458.6830	1.2732	0.0120
2454458.7226	1.2717	0.0112
2454458.7661	1.2652	0.0111
2454458.8135	1.2600	0.0111

Table 4—Continued

JD (1)	$F_{4.8GHz}$ -Jy (2)	σ (3)
2454521.3868	1.1271	0.0115
2454521.4216	1.1113	0.0110
2454521.4609	1.1093	0.0109
2454521.5033	1.1095	0.0109
2454521.5464	1.1213	0.0121
2454521.5937	1.1600	0.0129
2454521.6445	1.1538	0.0128
2454522.2182	1.0875	0.0110
2454522.2478	1.0768	0.0110
2454522.2824	1.0756	0.0108
2454522.3166	1.0689	0.0107
2454522.3510	1.0609	0.0106
2454522.3822	1.0827	0.0107
2454522.4170	1.0480	0.0104
2454522.4562	1.0415	0.0103
2454522.4986	1.0603	0.0104
2454522.5419	1.0433	0.0103
2454522.5890	1.0512	0.0107
2454523.2693	1.0286	0.0105
2454523.3081	1.0340	0.0103
2454523.3286	1.0346	0.0103
2454523.3597	1.0459	0.0103
2454523.3940	1.0349	0.0106
2454523.4331	1.0516	0.0105
2454523.4725	1.0491	0.0103
2454523.5183	1.0452	0.0103
2454523.5617	1.0590	0.0106
2454523.6090	1.0691	0.0111
2454523.6566	1.0753	0.0120
2454524.2070	1.0655	0.0107
2454524.2333	1.0752	0.0107
2454524.2696	1.0746	0.0106
2454547.1618	1.1102	0.0102
2454547.2026	1.1061	0.0098
2454547.2432	1.1197	0.0099
2454547.2775	1.1075	0.0098
2454547.3087	1.1248	0.0099
2454547.3433	1.1170	0.0098
2454547.4219	1.1001	0.0099
2454547.4570	1.1178	0.0098
2454547.4906	1.1226	0.0100
2454547.5350	1.1306	0.0101
2454547.5749	1.1179	0.0100
2454548.1677	1.0855	0.0099
2454548.2078	1.0964	0.0097

Table 4—Continued

JD (1)	$F_{4.8GHz}$ -Jy (2)	σ (3)
2454548.2484	1.0972	0.0097
2454548.2828	1.0796	0.0095
2454548.3143	1.0562	0.0094
2454548.3489	1.0607	0.0093
2454548.3881	1.0579	0.0094
2454548.4277	1.0682	0.0094
2454548.4628	1.0738	0.0095
2454548.5000	1.0794	0.0095
2454548.5369	1.0846	0.0096
2454548.5769	1.1086	0.0099
2454549.1363	1.0668	0.0096
2454549.1732	1.0726	0.0095
2454549.2059	1.0916	0.0097
2454549.2464	1.0830	0.0096
2454549.2808	1.0933	0.0097
2454549.3121	1.0917	0.0097
2454549.3284	1.0951	0.0096
2454549.3674	1.1098	0.0099
2454549.4068	1.0870	0.0096
2454549.4464	1.1103	0.0098
2454549.4800	1.0670	0.0095
2454549.5411	1.0718	0.0095
2454549.5810	1.0652	0.0097
2454578.1404	1.1811	0.0118
2454578.1790	1.1438	0.0109
2454578.2105	1.0327	0.0101
2454578.2453	1.1888	0.0114
2454578.2875	1.1577	0.0111
2454578.3304	1.1227	0.0116
2454578.3674	1.0111	0.0102
2454578.4439	1.0971	0.0107
2454578.4870	1.2260	0.0118
2454579.0844	1.1281	0.0112
2454579.1255	1.0614	0.0104
2454579.1664	1.0688	0.0104
2454579.1901	1.0183	0.0100
2454579.2567	1.1958	0.0113
2454579.3420	1.1753	0.0113
2454579.3788	1.1163	0.0108
2454579.4190	1.1267	0.0109
2454579.4590	1.0338	0.0108
2454579.5023	1.0245	0.0107
2454580.0682	1.1376	0.0113
2454580.1087	1.0735	0.0108
2454580.1843	1.1256	0.0110

Table 4—Continued

JD (1)	$F_{4.8GHz}$ -Jy (2)	σ (3)
2454580.2414	1.0303	0.0115
2454580.3634	1.0529	0.0109
2454580.4400	1.0784	0.0117
2454580.4831	0.9895	0.0106
2454581.0669	1.0734	0.0134
2454581.1102	1.0433	0.0109
2454581.1513	1.1218	0.0124
2454722.1092	2.9890	0.0273
2454722.6742	3.0528	0.0278
2454722.7005	3.0498	0.0278
2454722.7348	3.0426	0.0277
2454722.7691	3.0462	0.0277
2454722.8034	3.0473	0.0278
2454722.8347	3.0514	0.0278
2454722.8697	3.0514	0.0278
2454722.9090	3.0711	0.0280
2454722.9514	3.0705	0.0279
2454722.9914	3.0817	0.0280
2454723.0352	3.0924	0.0281
2454723.0821	3.0916	0.0281
2454723.6623	3.0860	0.0281
2454723.6922	3.1290	0.0285
2454723.7265	3.1410	0.0286
2454723.7607	3.1409	0.0286
2454723.7951	3.1450	0.0286
2454723.8264	3.1386	0.0286
2454723.8615	3.1681	0.0288
2454723.9007	3.1439	0.0286
2454723.9431	3.1599	0.0287
2454723.9811	3.1625	0.0287
2454724.0249	3.1760	0.0289
2454724.0687	3.1978	0.0291
2454724.1164	3.2080	0.0292
2454724.6574	3.2318	0.0294
2454724.6873	3.2239	0.0293
2454724.7216	3.2357	0.0294
2454724.7559	3.1992	0.0291
2454724.7902	3.2107	0.0292
2454724.8214	3.2038	0.0291
2454724.8561	3.1870	0.0290
2454724.8953	3.1842	0.0289
2454724.9348	3.1779	0.0289
2454724.9727	3.1860	0.0290
2454725.0128	3.1868	0.0290
2454725.0567	3.2073	0.0292

Table 4—Continued

JD (1)	$F_{4.8GHz}$ -Jy (2)	σ (3)
2454725.1004	3.2209	0.0293
2454752.6044	4.4033	0.0417
2454752.6478	4.3825	0.0415
2454752.6853	4.4016	0.0417
2454752.7231	4.4212	0.0418
2454752.7578	4.4438	0.0421
2454752.7926	4.4270	0.0419
2454752.8320	4.4343	0.0420
2454752.8745	4.4416	0.0420
2454752.9148	4.4518	0.0421
2454752.9588	4.4260	0.0419
2454753.0059	4.3679	0.0414
2454776.6563	5.1016	0.0615
2454776.6909	5.1441	0.0620
2454776.7258	5.1393	0.0619
2454776.7652	5.1569	0.0621
2454776.8077	5.1535	0.0621
2454776.8478	5.1533	0.0621
2454776.8916	5.1516	0.0621
2454776.9392	5.1452	0.0620
2454777.7109	5.2505	0.0633
2454777.7502	5.2839	0.0637
2454777.7898	5.2637	0.0634
2454777.8277	5.2611	0.0634
2454777.8678	5.2374	0.0631
2454777.9118	5.2200	0.0629
2454777.9558	5.1618	0.0622
2454778.5077	5.2032	0.0627
2454778.5419	5.2724	0.0636
2454778.5794	5.3162	0.0641
2454778.6169	5.3094	0.0640
2454778.6547	5.2871	0.0637
2454778.6895	5.3428	0.0644
2454778.7244	5.3631	0.0647
2454778.7639	5.3429	0.0645
2454778.8064	5.3633	0.0648
2454778.8466	5.3297	0.0642
2454778.8938	5.2239	0.0630
2454779.5482	5.1945	0.0627
2454779.5857	5.2133	0.0629
2454779.6233	5.2067	0.0628
2454779.6612	5.1394	0.0620
2454779.6958	5.1426	0.0620
2454779.7349	5.1706	0.0623
2454779.7744	5.2275	0.0631

Table 4—Continued

JD (1)	$F_{4.8GHz}$ -Jy (2)	σ (3)
2454779.8170	5.2449	0.0633
2454779.8572	5.2797	0.0637
2454779.9013	5.3242	0.0642
2454779.9453	5.3162	0.0641
2454822.5457	4.2800	0.0439
2454822.5803	4.2705	0.0438
2454822.6194	4.2735	0.0438
2454822.6589	4.2846	0.0439
2454822.7014	4.2803	0.0439
2454822.7416	4.2516	0.0436
2454822.7852	4.2462	0.0435
2454822.8292	4.2552	0.0436
2454823.3827	4.3162	0.0443
2454823.4167	4.2931	0.0440
2454823.4544	4.2997	0.0441
2454823.4919	4.3123	0.0442
2454823.5297	4.3301	0.0444
2454823.5645	4.3180	0.0443
2454823.5995	4.3406	0.0445
2454823.6388	4.3393	0.0445
2454823.6814	4.3516	0.0446
2454823.7215	4.3387	0.0445
2454823.7651	4.3372	0.0444
2454823.8122	4.3440	0.0445
2454824.3829	4.3042	0.0442
2454824.4172	4.2555	0.0436
2454824.4623	4.2482	0.0435
2454824.4999	4.2587	0.0437
2454824.5378	4.2759	0.0438
2454824.5724	4.2938	0.0440
2454824.5881	4.2853	0.0439
2454824.6316	4.2900	0.0440
2454824.6520	4.2949	0.0440
2454824.6946	4.2861	0.0439
2454824.7347	4.2595	0.0436
2454824.7788	4.2572	0.0436
2454824.8228	4.2553	0.0436
2455007.8902	1.9045	0.0200
2455007.9270	1.9247	0.0194
2455008.0084	1.9608	0.0209
2455008.0869	2.0382	0.0202
2455008.1294	1.9617	0.0191
2455008.1858	1.9404	0.0190
2455008.2290	1.9328	0.0190
2455008.2760	1.9136	0.0190

Table 4—Continued

JD (1)	$F_{4.8GHz}$ -Jy (2)	σ (3)
2455008.3228	1.9241	0.0189
2455008.8838	1.8863	0.0189
2455008.9206	1.8566	0.0184
2455008.9613	1.8686	0.0186
2455009.0018	1.8366	0.0182
2455009.0394	1.8657	0.0183
2455009.0804	1.9024	0.0185
2455009.1228	1.9014	0.0185
2455009.1684	1.9118	0.0186
2455009.2113	1.9116	0.0186
2455009.2585	1.9272	0.0188
2455009.3084	1.9407	0.0190
2455009.8752	1.9021	0.0186
2455009.9123	1.8923	0.0184
2455009.9528	1.8842	0.0183
2455009.9933	1.9160	0.0186
2455010.0309	1.8845	0.0183
2455010.0718	1.9103	0.0186
2455064.7658	1.5774	0.0156
2455064.8126	1.5812	0.0156
2455064.8605	1.5722	0.0155
2455064.8980	1.5629	0.0154
2455064.9365	1.5644	0.0155
2455065.7360	1.6155	0.0160
2455065.7789	1.5823	0.0159
2455065.8259	1.5543	0.0153
2455065.8698	1.5666	0.0154
2455065.9076	1.5623	0.0154
2455065.9431	1.5641	0.0154
2455065.9862	1.5699	0.0155
2455066.0327	1.5663	0.0155
2455066.0788	1.5811	0.0156
2455066.1242	1.5666	0.0155
2455066.1731	1.5814	0.0158
2455066.7264	1.5662	0.0156
2455066.7692	1.5736	0.0155
2455066.8162	1.5545	0.0153
2455066.8601	1.5558	0.0153
2455066.8979	1.5657	0.0154
2455066.9368	1.5414	0.0154
2455066.9797	1.5696	0.0154
2455067.0263	1.5779	0.0157
2455067.0724	1.5467	0.0152
2455067.1179	1.5387	0.0152
2455067.1666	1.5544	0.0155

Table 4—Continued

JD (1)	$F_{4.8GHz}$ -Jy (2)	σ (3)
2455067.7355	1.5000	0.0150
2455067.7793	1.5335	0.0153
2455067.8264	1.5266	0.0151
2455067.8706	1.5349	0.0151
2455067.9086	1.5117	0.0151
2455067.9501	1.5299	0.0151
2455067.9967	1.5335	0.0151
2455068.0426	1.5340	0.0151
2455068.0885	1.5333	0.0152
2455068.1338	1.5326	0.0152
2455096.6346	1.4986	0.0160
2455096.6651	1.5064	0.0161
2455096.7020	1.5159	0.0161
2455096.7364	1.5132	0.0160
2455096.7708	1.5113	0.0160
2455096.8023	1.5069	0.0160
2455096.8373	1.5008	0.0160
2455097.6385	1.4641	0.0157
2455097.6686	1.4538	0.0155
2455097.7031	1.4492	0.0154
2455097.7376	1.4855	0.0160
2455097.7866	1.4569	0.0155
2455097.8212	1.4668	0.0155
2455097.8565	1.4693	0.0156
2455097.8962	1.4679	0.0156
2455097.9390	1.4811	0.0157
2455097.9794	1.4871	0.0159
2455098.0236	1.4693	0.0156
2455098.0679	1.4815	0.0158
2455098.6466	1.4221	0.0153
2455098.6768	1.4436	0.0154
2455098.7113	1.4425	0.0153
2455098.7507	1.4380	0.0153
2455098.7850	1.4480	0.0155
2455098.8199	1.4348	0.0152
2455098.8597	1.4479	0.0153
2455098.8995	1.4315	0.0152
2455098.9424	1.4340	0.0152
2455098.9828	1.4314	0.0152
2455099.0268	1.4349	0.0153
2455099.6347	1.4831	0.0158
2455099.6922	1.4972	0.0159
2455099.7266	1.4991	0.0159
2455099.7611	1.5077	0.0160
2455099.7923	1.5119	0.0160

Table 4—Continued

JD (1)	$F_{4.8GHz}$ -Jy (2)	σ (3)
2455099.8272	1.5128	0.0160
2455099.8669	1.5170	0.0161
2455099.9067	1.5108	0.0160
2455099.9449	1.5296	0.0162
2455099.9853	1.5180	0.0161
2455100.0296	1.5283	0.0162
2455100.0750	1.5331	0.0164
2455100.6374	1.5076	0.0161
2455100.6676	1.4986	0.0159
2455100.7020	1.4898	0.0158
2455100.7364	1.4980	0.0159
2455100.7709	1.4904	0.0158
2455100.8025	1.4874	0.0158
2455100.8374	1.4892	0.0158
2455100.8772	1.4688	0.0156
2455100.9200	1.4625	0.0155
2455100.9604	1.4513	0.0154
2455101.0045	1.4542	0.0154
2455101.0488	1.4607	0.0155
2455101.6812	1.4323	0.0152
2455101.7156	1.4373	0.0153
2455101.7500	1.4469	0.0153
2455101.7813	1.4581	0.0154
2455101.8161	1.4731	0.0156
2455101.8556	1.4742	0.0156
2455101.8954	1.4742	0.0156
2455101.9382	1.4707	0.0156
2455101.9787	1.4685	0.0156
2455102.0229	1.4686	0.0157
2455102.0673	1.4815	0.0158
2455113.5992	1.4880	0.0156
2455113.6293	1.4886	0.0155
2455113.6667	1.4735	0.0153
2455113.7041	1.4685	0.0152
2455113.7417	1.4787	0.0153
2455113.7762	1.4737	0.0152
2455113.8143	1.4756	0.0152
2455113.8571	1.4590	0.0151
2455113.9028	1.4688	0.0152
2455113.9461	1.4506	0.0150
2455113.9932	1.4541	0.0151
2455114.0414	1.4577	0.0152
2455114.6174	1.4519	0.0151
2455114.6547	1.4556	0.0151
2455114.6921	1.4500	0.0150

Table 4—Continued

JD (1)	$F_{4.8GHz}$ -Jy (2)	σ (3)
2455114.7297	1.4568	0.0151
2455114.7502	1.4618	0.0151
2455114.7879	1.4567	0.0151
2455114.8302	1.4464	0.0150
2455114.8732	1.4510	0.0150
2455114.9163	1.4397	0.0149
2455114.9633	1.4443	0.0150
2455115.0146	1.4453	0.0150
2455157.5039	1.2476	0.0166
2455157.5549	1.2636	0.0167
2455157.6057	1.2636	0.0166
2455157.6528	1.2689	0.0167
2455157.7055	1.2743	0.0168
2455157.7589	1.2540	0.0164
2455157.8065	1.2446	0.0164
2455157.8502	1.2625	0.0166
2455157.8979	1.2401	0.0164
2455158.4868	1.2459	0.0164
2455158.5243	1.2882	0.0170
2455158.5753	1.2632	0.0166
2455158.6260	1.2457	0.0163
2455158.6743	1.2585	0.0167
2455158.7275	1.2485	0.0165
2455158.7810	1.2604	0.0166
2455158.8250	1.2541	0.0165
2455158.8687	1.2730	0.0168
2455158.9166	1.2350	0.0164
2455159.5389	1.2370	0.0163
2455159.7552	1.2429	0.0163
2455159.8029	1.2499	0.0164
2455159.8465	1.2586	0.0166
2455159.8943	1.2431	0.0164
2455160.4788	1.2465	0.0164
2455160.5162	1.2421	0.0163
2455160.5670	1.2457	0.0163
2455160.6176	1.2405	0.0162
2455160.6657	1.2420	0.0163
2455160.7186	1.2369	0.0162
2455160.7719	1.2444	0.0164
2455160.8158	1.2413	0.0163
2455160.8615	1.2278	0.0161
2455160.9091	1.2252	0.0162
2455215.5453	1.2437	0.0140
2455215.6010	1.2526	0.0141
2455215.6535	1.2355	0.0139

Table 4—Continued

JD (1)	$F_{4.8GHz}$ -Jy (2)	σ (3)
2455215.6991	1.2359	0.0139
2455215.7482	1.2273	0.0139
2455215.7971	1.1990	0.0139
2455216.3199	1.2554	0.0142
2455216.3657	1.2699	0.0143
2455216.4221	1.2631	0.0142
2455216.4748	1.2620	0.0142
2455216.5257	1.2737	0.0143
2455216.5813	1.2603	0.0142
2455216.6341	1.2509	0.0141
2455216.6797	1.2284	0.0138
2455216.7289	1.2307	0.0139
2455216.7778	1.2612	0.0144
2455217.2994	1.2295	0.0140
2455217.3452	1.2322	0.0139
2455217.4017	1.2465	0.0140
2455217.4580	1.2471	0.0140
2455217.5090	1.2474	0.0140
2455217.5239	1.2499	0.0141
2455217.5796	1.2330	0.0139
2455217.6360	1.2141	0.0137
2455217.6815	1.2225	0.0137
2455217.7306	1.2177	0.0137
2455217.7794	1.2160	0.0140
2455218.3232	1.2589	0.0142
2455218.3736	1.2458	0.0140
2455218.4296	1.2555	0.0141
2455218.4823	1.2651	0.0142
2455218.5377	1.2554	0.0141
2455218.5786	1.2403	0.0139
2455218.6311	1.2338	0.0139
2455218.6765	1.2295	0.0138
2455218.7256	1.2261	0.0138
2455218.7742	1.2427	0.0143